energies

Review

In-Wheel Motor Drive Systems for Electric Vehicles: State of the Art, Challenges, and Future Trends

Kritika Deepak [1,2], Mohamed Amine Frikha [1,2], Yassine Benômar [1,2], Mohamed El Baghdadi [1,2] and Omar Hegazy [1,2,*]

[1] MOBI-EPOWERS Research Group, ETEC Department, Vrije Universiteit Brussel (VUB), 1050 Brussels, Belgium; kritika.deepak@vub.be (K.D.)
[2] Flanders Make, Gaston Geenslaan 8, 3001 Heverlee, Belgium
[*] Correspondence: omar.hegazy@vub.be

Abstract: Recently, there has been significant attention given to the electrification of transportation due to concerns about fossil fuel depletion and environmental pollution. Conventional drive systems typically include a clutch, reduction gear, and mechanical differential, which results in power loss, noise, vibration, and additional maintenance. However, in-wheel motor drive technology eliminates the need for these components, providing benefits such as higher system efficiency, improved wheel control, and increased passenger comfort. This article offers a comprehensive review of the technology and development of in-wheel motor drives. It begins with an overview of in-wheel motor drives in electric vehicles, followed by an exploration of the types of electric motors suitable for in-wheel motor drives. The paper then presents an industrial state of the art of in-wheel motors, comparing them with conventional motor drives, and reviews the implemented power electronics, control system, and cooling systems. Finally, the paper concludes by providing an outlook on the challenges and future trends of in-wheel drive systems.

Keywords: in-wheel motors; axial flux motors; outer-rotor PMSM motors; rare earth elements; unsprung mass; torque distribution

Citation: Deepak, K.; Frikha, M.A.; Benômar, Y.; El Baghdadi, M.; Hegazy, O. In-Wheel Motor Drive Systems for Electric Vehicles: State of the Art, Challenges, and Future Trends. *Energies* **2023**, *16*, 3121. https://doi.org/10.3390/en16073121

Academic Editors: Pedro Roncero-Sanchez, Trung Van Nguyen, João Paulo Carvalho Lustosa da Costa, Caiping Zhang, Kaamran Raahemifar and Roberto Villafafila-Robles

Received: 25 February 2023
Revised: 21 March 2023
Accepted: 23 March 2023
Published: 29 March 2023

1. Introduction

Over the past few decades, there has been widespread attention given to the issues of energy crises and environmental pollution. The global community has recognized the urgency of conserving energy and reducing emissions, as indicated by the research in [1,2]. Electrification has emerged as an alternative solution for various industrial applications, particularly in the realm of transportation, where electric vehicles have shown promise. Thanks to advances in high-performance electric motors and power electronics, electric and hybrid electric vehicles (EVs/HEVs) are being developed and studied as a substitute for conventional internal combustion engines (ICE) automobiles [3]. The Tesla Model 3, Renault Zoe, Volkswagen ID3, and Volkswagen ID4 are currently the most popular EVs in the european market [4–7]. However, the conventional central-motor drive system in EV/HEV involves linking the propulsion motor to the wheels via a chain of mechanical transmission components [8,9]. Unfortunately, this mechanical transmission setup leads to increased weight and higher maintenance costs [10]. Alternatively, an in-wheel motor (IWM) could be used to directly power the wheels without the use of mechanical transmission. Placing the motor inside the wheel rim allows for the speed and torque output of the motor to be directly transmitted to the wheel. Consequently, IWMs operate at lower speeds but with higher torque when compared to central-motor drives. This method provides numerous benefits, including increased space for passengers and batteries, as well as greater control flexibility through independent wheel control [11].

Over a hundred years ago, in 1900, the first-ever IWM driven automobile was created by Lohner–Porsche Electromobile [12]. This vehicle was propelled by two IWMs, which were powered by a forty-four cell 80-volt lead battery [13]. Later, Porsche also introduced the first functional hybrid car, using a combustion engine to drive the generator and supply power to the wheel hub motor. This car failed over the years as it weighed almost two tonnes [12]. Electric cars and gasoline-powered cars were in significant competition for a period of time. Nonetheless, the introduction of Henry Ford's Model T in 1908 led to a shift in favor of gasoline-powered vehicles, ultimately resulting in greater affordability at a larger scale. In the following years, electric vehicles were outperformed by ICE vehicles.

The contemporary fascination with electric vehicles can be traced back to the release of the Toyota Prius in 1997, which was the world's first mass-produced hybrid electric vehicle. This event sparked interest in modern electric vehicles in the automobile market. Moreover, the US Department of Energy states that electric vehicles are highly energy efficient as they convert more than 77% of electrical energy into power that drives the wheels. In stark contrast, gasoline-powered vehicles convert only 11% to 37% [3] of the energy stored in gasoline into kinetic power. Additionally, the rising global awareness and concern for environmental impact of combustion vehicles fueled by oil is drawing consumers to go electric.

This review article critically evaluates the technology and advancements of IWM drives by thoroughly analyzing existing research studies and data. The authors compared the benefits and design requirements of IWM drives and present a comprehensive overview of their use in electric cars. Authors also explored various types of electric motors used in IWM drives and their compliant features, potential, and further enhancements. Furthermore, the authors examine the industrial state of the art of IWM drives and compare them to conventional motor drives. There are many engineering topics and issues involved in the design of an IWM, such as electromagnetic performance, power electronics, motor and vehicle control strategies, thermal management and cooling systems, vibration, unsprung mass, and structural challenges, and several individual studies have been conducted to optimize them. However, there is a research gap in the combined knowledge of these topics. Therefore, the authors have highlighted the main techniques and research methodologies of all relevant topics related to IWM technology. The authors conclude by identifying potential areas for future advancements and challenges that need to be addressed to make IWM technology more usable.

1.1. In-Wheel Motor Drives vs. Central-Motor Drives

When using an IWM-driven electric vehicle (IWM-DEV), all four wheels can be independently driven by the motor and the motion of each wheel can be completely autonomous without any rigid mechanical connection between them, as shown in Figure 1. This design leads to a significant weight reduction, structural simplification, and vehicle range improvement. Therefore, IWM-DEVs drive is considered the most viable form of drive for EVs. Since the torque of each wheel can be controlled independently, the vehicle can be easily integrated with individual inverter and its control unit, and vehicle steering control systems. This provides a greater number of controllable degrees of freedom compared to traditional ICE vehicles, making it an ideal platform for the latest vehicle control technology and for achieving optimal vehicle dynamics.

Central-motor drives have several disadvantages over IWM [14]:

1. A larger number of components introduced from transmission;
2. Over 10% of vehicle weight is contributed due to transmission components;
3. 15% losses contributed from transmission and slip efficiency;
4. Decreased space for passenger, cargo, and battery.

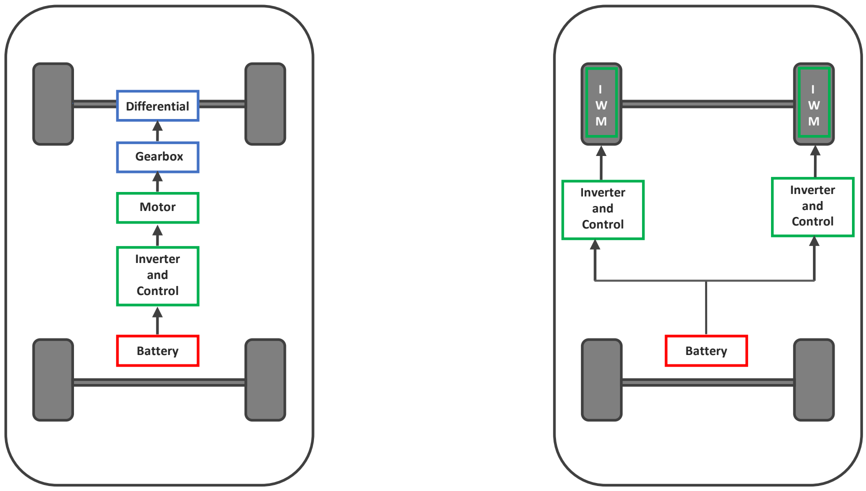

(**a**) Central motor drive vehicle architecture (**b**) IWM drive vehicle architecture

Figure 1. Vehicle architecture of (**a**) central-motor driven EV (**b**) IWM drive EV.

Compared to the conventional central-motor drive system, IWM-DEVs offer various advantages such as higher system efficiency, reduced mechanical maintenance, and increased onboard storage space. Moreover, the independent control of each wheel enables adaptable handling for different road conditions. Nonetheless, the IWM-drive system has a significant drawback in the form of increased unsprung mass resulting from the propulsion motor being integrated into the wheel. As the motor needs to transfer a similar amount of power at a much lower operating speed, a larger and more complex motor design is required. Therefore, IWM-DEVs have not been utilized in mass-produced commercial EV/HEV, and further research is necessary to overcome this challenge. In order to design a motor as suitable as IWM, the following requirements must be considered [15–18]:

1. Compact structure with short axial length;
2. Largest possible diameter of airgap for a given wheel size. Outer rotor topologies are suitable;
3. High efficiency at lower speeds as the wheel is driven directly by the motor without reduction gearbox;
4. High torque density; achieved through by utilizing high pole pair number;
5. Light weight to reduce unsprung mass;
6. Robust and fault tolerant to endure the aggressive and harsh operating environment of IWM.

1.2. State of the Art in Central-Motor Drive EVs

Several electric machines have undergone comprehensive evaluations and comparisons in terms of power density, torque density, types of motor used etc, for their potential in EV traction applications. The trend of gravimetric power densities (GPD) [kW/kg] of the motor used in central-motor drive EVs over the years is shown in Figure 2. Toyota Prius was one of the first popular EVs that sparked the interest of consumers in EVs. The 2004 version of Prius used an internal permanent magnet synchronous mootor (IPMSM) with 50 kW and 400 N m with GPD of 1.11 kW/kg. As seen in Figure 2, the GPD has been increasing significantly since 2016. Lucid Air, introduced in 2022, has an electric motor that weighs only 31 kg, producing 500 kW [19]. The complete drive unit comprises an electric motor, inverter, reductions gearset, and differential, which collectively weighs 74 kg. Table 1 lists the specifications of the central-motor drives available for electric traction. It can be noted the motor angular speed of some motors can reach over 18,000 RPM.

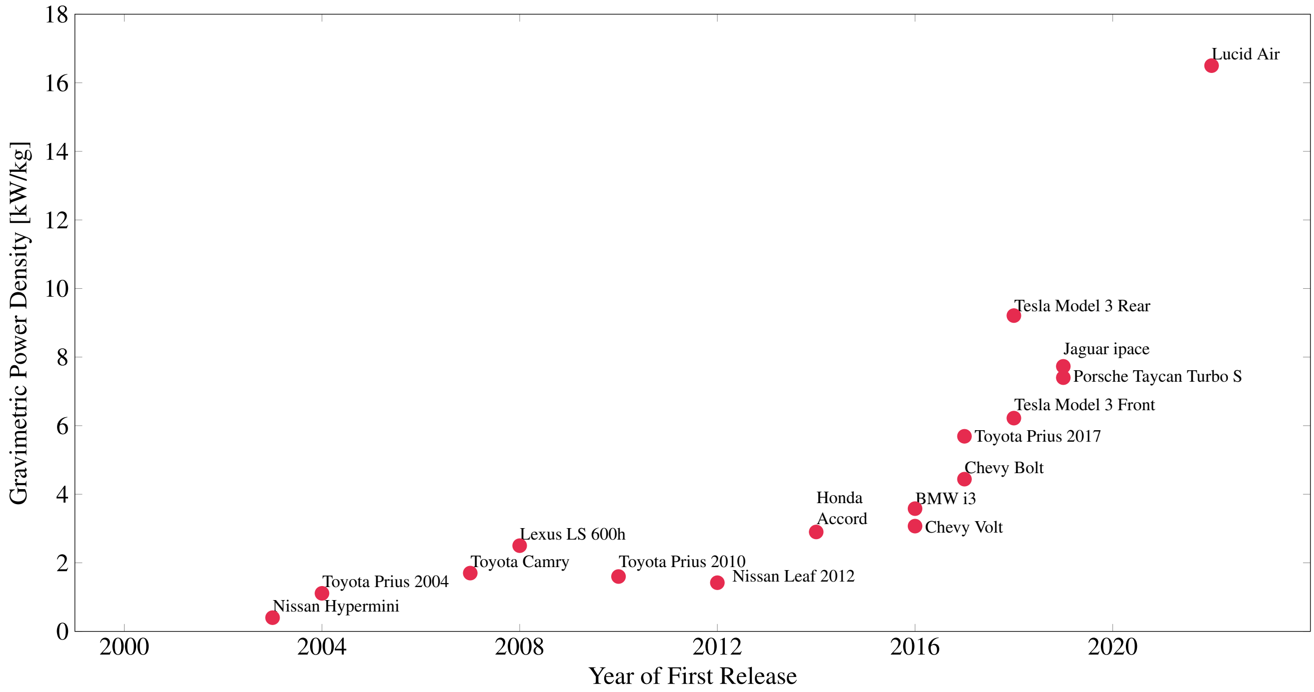

Figure 2. Gravimetric power density trend over the years of high-speed electric motors used in EVs [4,19–21].

Table 1. Specifications of commercially central-motor drives for electric traction [4,19–21].

	Motor Type	Power [kW]	Torque [Nm]	Speed (Peak) [RPM]
Nissan Hypermini	IPMSM	24	130	6700
Toyota Prius 2004	IPMSM	50	400	6000
Toyota Camry	IPMSM	70	270	14,000
Lexus LS 600h	IPMSM	110	300	10,230
Toyota Prius 2010	IPMSM	60	207	14,000
Nissan Leaf 2012	PMSynRM	80	280	10,390
Honda Accord	IPMSM	125	110	8000
Chevy Volt	PMSynRM	112	400	-
BMW i3	PMSynRM	125	250	11,400
Chevy Bolt	PMSynRM	150	360	8810
Toyota Prius 2017	PMSynRM	53	-	17,000
Tesla Model 3 Front	IM	145	-	18,100
Tesla Model 3 Rear	PMSynRM	285	-	18,100
Porsche Taycan Turbo S	PMSynRM	560	-	-
Jaguar i-pace	PMSynRM	294	696	13,000
Lucid Air	IPMSM	500	-	-

2. Motor Topologies for IWMs

This section presents a detailed overview of motor topologies suitable for IWM-DEVs, which are classified based on how magnetic flux lines travels through the motor. The two categories are radial flux motors (RFM) and axial flux motors (AFM), which are illustrated in Figure 3. In RFMs (Figure 3a), the rotor is nested cylindrically within the stator (or vice versa for an outer-rotor RFM), and the magnetic flux lines travels radially between stator and rotor. In contrast, in AFMs (Figure 3b) the stator and rotor are stacked axially and the magnetic flux travels axially along the shaft axis.

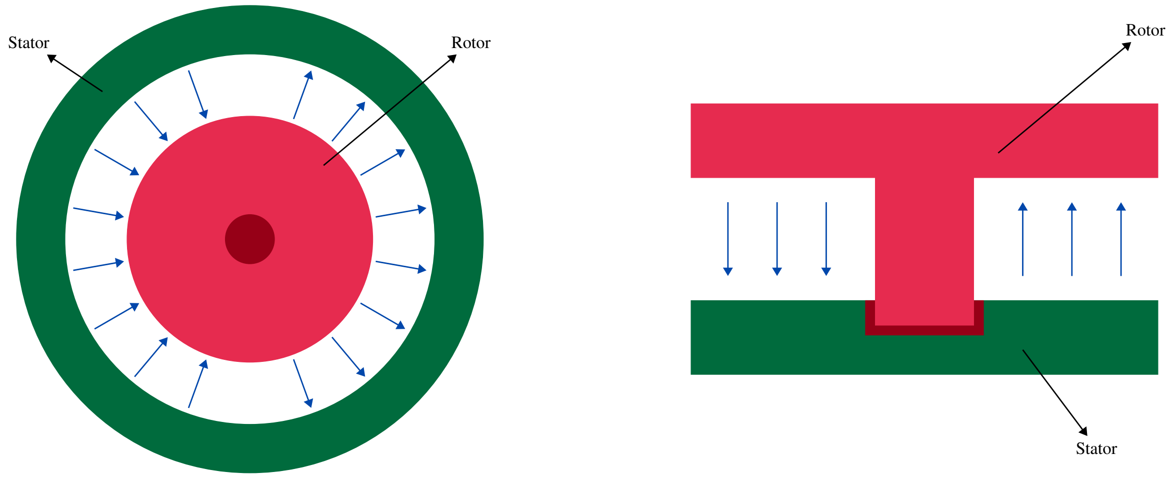

(**a**) Magnetic flux path in RFM (radial view)

(**b**) Magnetic flux path in AFM (axial view)

Figure 3. Magnetic flux is produced (**a**) radially along the rotor in RFM (**b**) axially along the axis of rotor in AFM.

2.1. Radial Flux Motors

2.1.1. Topologies of Radial Flux Motors in IWMs

A classification of RFM based on synchronous speed and excitation material (such as permanent magnets (PM)) is shown in Figure 4.

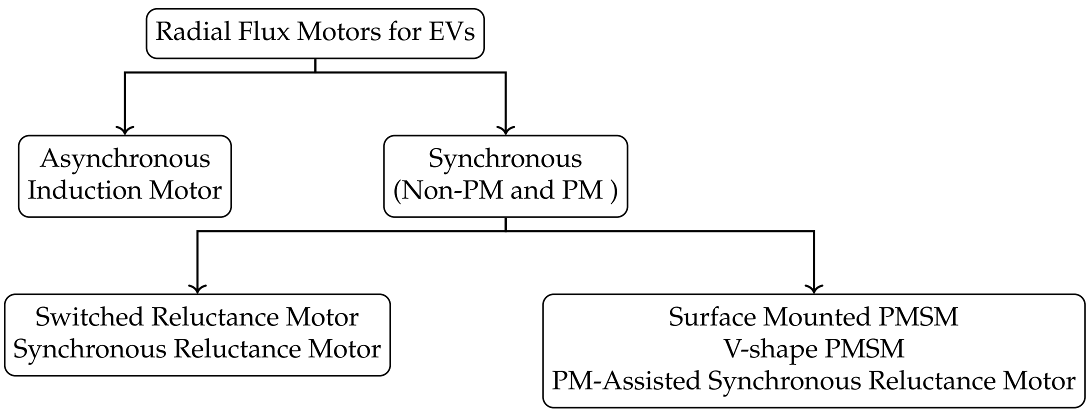

Figure 4. Radial flux motors' classification based on synchronous behavior of the motors. Synchronous motors are further classified based on the usage of magnets.

Permanent Magnet Synchronous Motors

The outer-rotor PMSM (OR-PMSMs) with neodymium PMs are a conventional choice of motor designers both in research and industrial sector for IWM-drive applications due to their high torque density. Fractional slot-concentrated winding is the preferableoption to accommodate an in-wheel installation, and opting for a high pole count results in a slimmer iron yoke design, ultimately reducing both weight and size [22,23]. The advantages of concentrated windings, such as enhanced fault tolerance and streamlined manufacturing, are well-documented in the literature [24,25]. Additionally, incorporating a multi-phase design can further improve fault tolerance. Certain OR-PMSM models include sub-motors to increase fault tolerance, and various techniques have been implemented to mitigate parasitic effects, such as eddy currents and NVH [17,26]. Two topologies based on the radial flux outer-rotor PMSM are shown in Figure 5, surface mounted PMSM with outer rotor (Figure 5a) and V-shaped IPM-PMSM (Figure 5b).

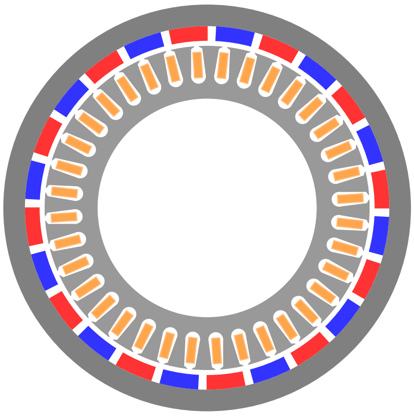

(**a**) Surface mounted outer rotor PMSM

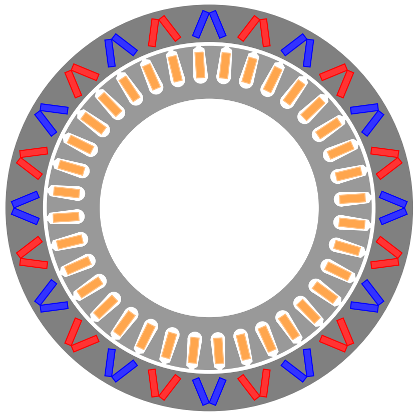

(**b**) V-shaped PM outer rotor PMSM

Figure 5. Motor topology of (**a**) Surface-mounted OR-PMSM (**b**) V-shaped Interior PM OR-PMSM.

Switched Reluctance Motor

The outer-rotor switched reluctance machine (OR-SRM) as shown in Figure 6 is a potential non-PM option for IWM-DEVs [27]. While it offers low cost, compact size, and a robust structure, due to the high magnetic saturation present in both the stator and rotor steel, the flux characteristics of the machine are non-linear [28]. As a result, the machine's efficiency is reduced and its torque performance is inferior to PMSM [29]. In [30] proposed a motor that combines the advantage of multiple teeth per stator pole and more rotor poles than stator teeth to achieve the purpose of enhancing the specific torque. The structure of two teeth can improve the output torque. Increasing the number of rotor poles results in a larger slot area for winding and allows a larger excitation current. However, the OR-SRM produces high pulsating torque, vibration, and noise, making it less desirable for IWM-drive applications. Researchers have employed multiphysics modeling and improved control methods to address these NVH issues [31,32].

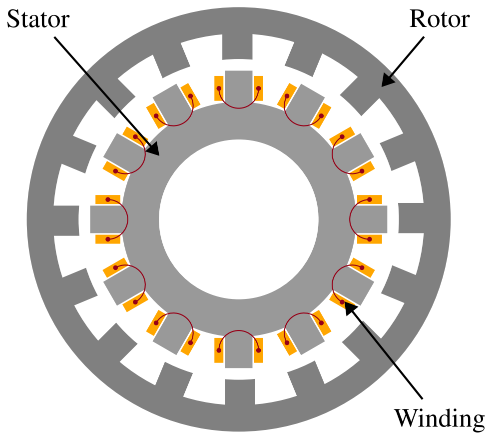

Figure 6. Topology of an outer-rotor switched reluctance motor.

Synchronous Reluctance Motor

Outer-rotor synchronous reluctance motors (OR-SynRM) are an under-explored class of motors for use as IWMs. Their torque ripple is smaller and they are quieter than OR-SRM. They also have higher efficiency than OR-SRM [33]. Figure 7 illustrates the topology of a OR-SynRM. Unlike OR-SRM, OR-SynRM can utilize the same stator as the PMSM motor. A sizing and design procedure of OR-SynRM is presented in [34] to optimize the flux barrier shape and rotor and stator size. The study took into account the structural analysis to ensure the rotor with flux barriers can withstand the stress at higher speeds. A PM-assisted

OR-SynRM is presented in [35] for IWM applications. A novel dual-rotor SynRM [36] is designed and compared with a single rotor counterpart. The dual rotor motor showed higher power density and lower torque ripple when compared to a single rotor. The above mentioned research developed OR-SynRM with maximum power 5 kW, hence more research investigation is required to develop high power OR-SynRM for IWM-DEVs.

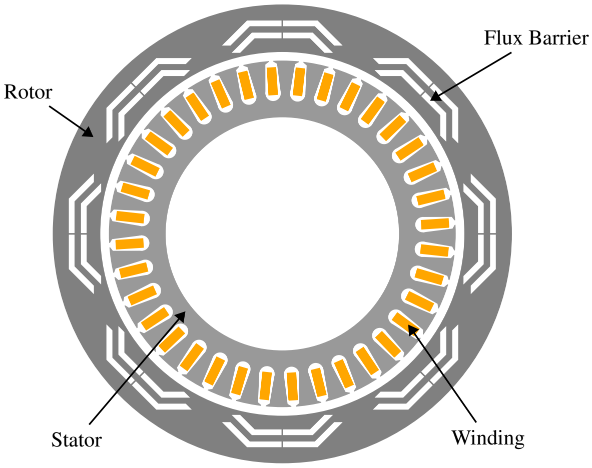

Figure 7. Topology of an outer-rotor synchronous reluctance motor.

Induction Motor

While PM-based motors are currently the preferred choice for traction applications, induction motors (IMs) have historically been favored for industrial applications due to their robustness and low-cost and as the price of rare-earth materials has risen sharply, there have been efforts to develop IMs for use in electric traction applications [29,37]. The topology of a squirrel cage type outer rotor induction machine (OR-IM), is shown in Figure 8, which can be utilized for IWM-applications [38]. However, the power range is comparatively very low in the proposed topologies, ranging up to only 6 kW [39].

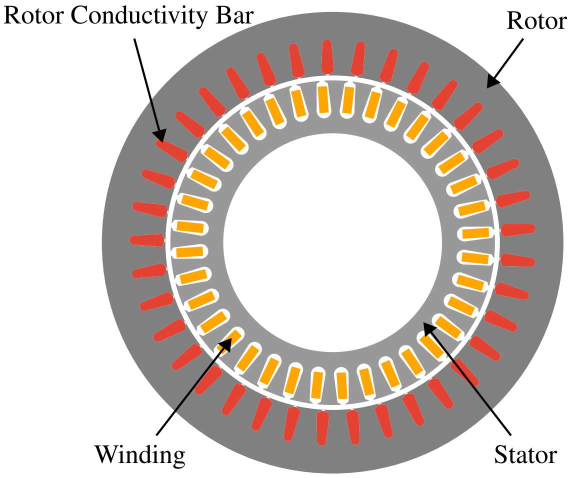

Figure 8. An outer-rotor induction motor topology.

Induction motors with distributed windings are the most prevalent, but their winding configuration is not favored due to the larger overall size of the machine and reduced magnetic core utilization, which is a huge limitation for IWM application [40]. In [41], a stator design with auxiliary slots and variable turns per coil is utilized to mitigate the spatial harmonics of the MMF. However, this approach entails a complex manufacturing process. In [42,43], the toroidal winding is proposed as a solution for reducing end-winding length in OR-IM. This enables the use of a startup strategy that entails a brief period of high current, resulting in lower power consumption. However, toroidal windings have some drawbacks: the winding process is complex and labor-intensive, which can lead to increased manufacturing costs and longer lead times and high leakage inductance, which can result in increased power loss and reduced motor performance [44].

2.1.2. Industrial State of the Art in Radial Flux Motors for IWMs

The industrial sector is dominated by outer-rotor PMSM motors for IWM applications. This is due to the high torque density owing to the rare earth PMs used in them. The trend shows that intensive research is required for torque dense motors without using RE magnets to compete in the industry. Table 2 lists the specifications of some commercial outer-rotor PMSM IWMs for automotive applications.

Table 2. Comparison of commercial radial flux IWM with PM.

	Unit	Protean Pd18	Elaphe L1500	PMW Dynamics XR32-13	GEM Motors G3
DC Link Voltage	V	400	370	100	48
Continuous Torque	Nm	650	650	300	370
Peak Torque	Nm	1250	1500	577	500
Continuous Power	kW	60	77	5.87	15
Peak Power	kW	80	110	-	20
Maximum Speed	RPM	1600	1480	2000	1000
Peak Efficiency	[%]	93	-	-	91
Mass	kg	36	34.8	32	27
Cooling	-	Water	Water	Water	Forced Air
References		[45]	[46]	[47]	[48]

Elaphe has developed four IWM in their portfolio: S400, M700, M1100, and L1500. S400 is designed for light weight EV and HEVs and can operate at 48 V and 100 V DC link voltage providing 400 N m peak torque and maximum speed of 750 RPM and 1565 RPM at 48 V and 100 V, respectively. Elaphe's M700 is suitable for medium weight passenger cars with peak torque 700 N m and maximum speed 1500 RPM. M1100 provides peak torque 1100 N m and maximum speed 1160 RPM. The most powerful in the range is L1500, with a peak torque of 1500 N m and peak power of 110 kW. Lordstown Motor uses Elaphe's L1500 in their all-electric pickup truck, making it the first commercially available EV driven with IWM [49,50]. All the motors are liquid cooled and utilizes NdFeB magnets for high torque density. The motor topology is outer-rotor PMSM [46].

2.2. *Axial Flux Motors*

Radial flux machines have been more popular since the beginning of electric motors' origin, and overshadowed the axial flux machines. This is partly because axial flux machines are more complicated to manufacture and operate. The intense magnetic force along the axis between the stator and rotor can cause the rotor discs to bend, and the production process can be difficult due to factors such as slotted stator lamination, high expenses, and challenges in assembling the various parts [51]. However, recent trends have shown that the features of axial motors are extremely favourable for IWM-DEVs, such as compact axial length, high torque density and flexible structure [52]. Despite extensive research on the topologies of axial flux machines, there are still gaps in their practical use and certain aspects of their analysis and design that need further exploration. To mitigate uncertainties related to rare-earth materials, there is ongoing research on developing non-rare-earth AFMs for IWM-DEVs. An axial flux switched-reluctance motor (AF-SRM) has beendeveloped for use in IWM-DEVs. This motor has a higher torque density than its radial flux counterpart. Additionally, the inherent problem of high pulsating torque can be addressed by using a double-rotor structure. AFMs and RFMs require different materials due to the difference in direction of the flux. Non-oriented grain electric steel and amorphous soft material are commonly used in AFMs [53].

The axial flux motors has the following advantages:

1. Compact structure, especially short axial sizes which is ideal for IMW technology;
2. Small stator core volume, therefore reduced stator core loss;
3. Low weight;
4. High torque density;
5. High power density;
6. Flexible and modular structure; motors can be stacked axially to increase the torque and power;
7. Small end-winding hence lower copper losses.

Disadvantages of axial flux motors:

1. Manufacturing and assembly problems due to complicated structure;
2. Higher cost;
3. Prone to non-uniform airgap due to strong axial magnetic forces between stator and rotor.

2.2.1. Topologies of Axial Flux Motors

Figure 9 shows the classification of axial flux-motor topologies based on the rotor and stator axial placement. According to the number of stator and rotor used and their relative position in the motor structure, the axial flux motors are categorized as single-stator single-rotor (SSSR), single-stator double-rotor (SSDR), double-stator single-rotor (DSSR), and multi-stator multi-rotor (MSMR). Like radial flux motors, the rotor of axial flux motors can either be permanent magnet (PM-based) or induction motors.

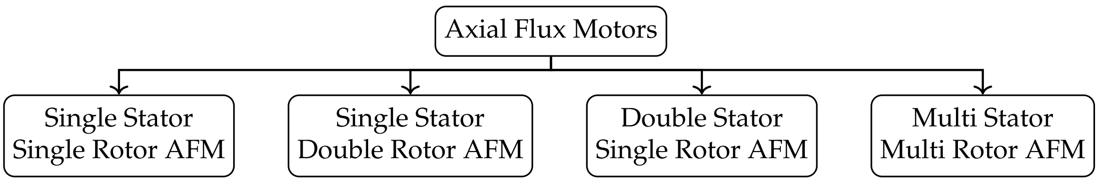

Figure 9. Axial Flux Motors classification.

Single-Stator Single-Rotor (SSSR)

The single-stator single-rotor (SSSR) configuration is the most basic structure of AFMs. Due to their compact size and high torque capacity, SSSR-type AFMs are widely utilized in the servo drive, gearless elevators, and transportation industries [54]. However, the unbalanced axial force between the stator and rotor can cause structural deformation, generate vibration noise, and shorten the motor's lifespan [55]. To achieve maximum rotational torque while minimizing axial force, several techniques have been proposed, including adjusting the portions of stator winding currents, utilizing complex bearing arrangements, using a thicker rotor disc, and implementing a current shifting angle [56].

Single-Stator Double-Rotor (SSDR)

AFM motors of the single-stator double-rotor (SSDR) type, which feature a slotted or slotless stator positioned between two rotors, exhibit excellent symmetry that effectively cancels out unbalanced axial forces. As a result, the motor's vibration and lifespan can be improved over its lifecycle. Slotless machines are particularly advantageous because their end windings are shorter, resulting in lower copper loss and better heat dissipation. In addition, leakage and mutual inductance are reduced in slotless configurations, resulting in the elimination of slot effects such as flux ripple, cogging torque, high-frequency rotor loss, and stator teeth. This configuration is highly suitable for IWMs [57]. A SSDR type axial flux induction motor is designed in [58] to eliminate the magnetic axial force between the rotor and stator. The rotor design was optimized to reduce the torque ripple by introducing the skewing and rotational displacement of rotors, which also increases the power factor of the motor as well.

Double-Stator Single-Rotor (DSSR)

In double-stator single-rotor (DSSR) AFM motors, the rotor is sandwiched between two stators. The permanent magnet (PM) can be positioned on the surface or inside the rotor. Inserting the PM inside the rotor provides better protection against shock and corrosion compared to the surface-mounted PM structure [59]. The power density of the interior permanent magnet (IPM) structure is lower than that of the surface-mounted structure due to the need for a thicker rotor disc. Additionally, the leakage flux of PM ends and armature reactions are higher in the interior design due to the PMs being surrounded by ferromagnetic material. A DSSR can have either a slotted stator (SS type) or a slotless stator (NS type) configuration, with the rotor situated between the two stators. A DSSR-type axial flux switched-reluctance motor was used by [60] for IWM applications. The axial flux switched-reluctance motor has the advantage of magnetic force equalization in terms of stator balance compared SSSR, the existence of two stators results in two air gaps and a reduced peak inductance, leading to a lower power density.

Multi-Stator Multi-Rotor (MSMR)

MSMRs, also referred to as multi-stage AFPM machines, can be built using either DSSR or SSDR configurations. The MSMR-type AFPM motors consist of N stators and (N+1) rotors, enabling them to achieve higher torque and power density without an increase in motor diameter. These motors are well-suited for high-torque applications, such as ship propulsion. The stator windings of AFPM and RFPM machines can be connected in either parallel or series. In a multi-stage configuration, the torque and power density are improved without increasing the diameter of the machine. Compared to RFPM machines, multi-stage AFPM machines are easier to assemble due to their planar air gap [61].

2.2.2. Industrial State of the Art in Axial Flux Motors

YASA has created motors with a yokeless and segmented armature design, as shown in Figure 10. YASA 750R motor can produce a peak power density of >5 kW/kg, peak torque density >75 Nm/L with peak efficiency of >95% at its highest point [62]. The YASA design eliminates the torque ripple caused by stator slotting and reduces the mass of the motor. However, due to a longer airgap length, the winding inductance is lower, resulting in a reduced flux-weakening capability [63].

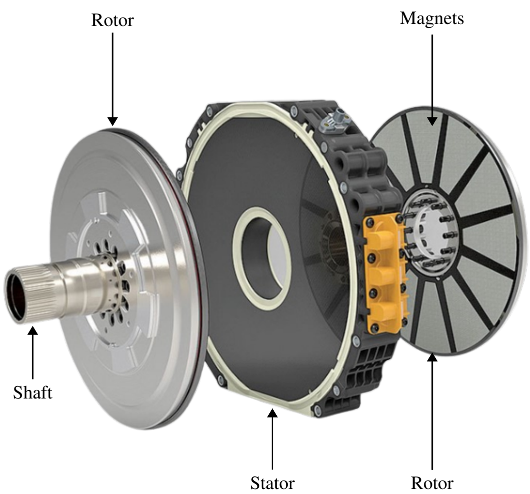

Figure 10. YASA axial flux motor [62].

Avid Technologies, now acquired by Turntide technologies [64], produces highly efficient AFM for DC link operating voltage up to 800 V. Magnax provides an axial flux motor with high peak power density of 12.5 [kW/kg]. Emrax provides axial flux motors with 100–1000 Nm for both automotive and aerospace applications, as shown in Table 3.

Table 3. Comparison of commercial radial flux motor with permanent magnets.

	Unit	YASA 750R	Magnax AXF275	Turntide EVO AF130	EMRAX 208
DC Link Voltage	[V]	700	-	600	580
Continuous Torque	[Nm]	400	260	145	90
Peak Torque	[Nm]	790	520	350	150
Continuous Power	[kW]	70	150	64	56
Peak Power	[kW]	100	300	140	86
Maximum Speed	[RPM]	3250	8000	8000	7000
Peak Efficiency	[%]	-	95	98	96
Peak Power Density	[kW/kg]	5	12.5	10	8.3
Mass	[kg]	37	24	30.5	10.3
Cooling	-	Water-Cooled	Water-Cooled	Water/Glycol Cooled	Air + Water
References		[62]	[65]	[66]	[67]

Figure 11 shows a power trend comparison of commercially available IWMs for EVs. It can be noticed that some central-motor drives, such as the Porsche Taycan Turbo S, can provide an extremely high over-boost power of 560 kW but at the cost of high mass (76 kg) [21]. A general trend of high power with lower mass can be seen in axial flux IWMs. Motors such as Magnax AXF275, Turntide, and EMRAX motors [65–67] have also claimed to have peak efficiency over 95% with high power densities. Because of their shorter magnetic path, AFMs can produced a higher torque than RFMs [68]. IWMS have stricter requirements in terms of space as they need to fit in the wheel hub, hence their outer diameter and axial length is limited, affecting their torque/power capabilities directly. Research focused on the optimization of the motor geometrical parameters and cooling system to increase the torque capability and minimize the losses needs more attention.

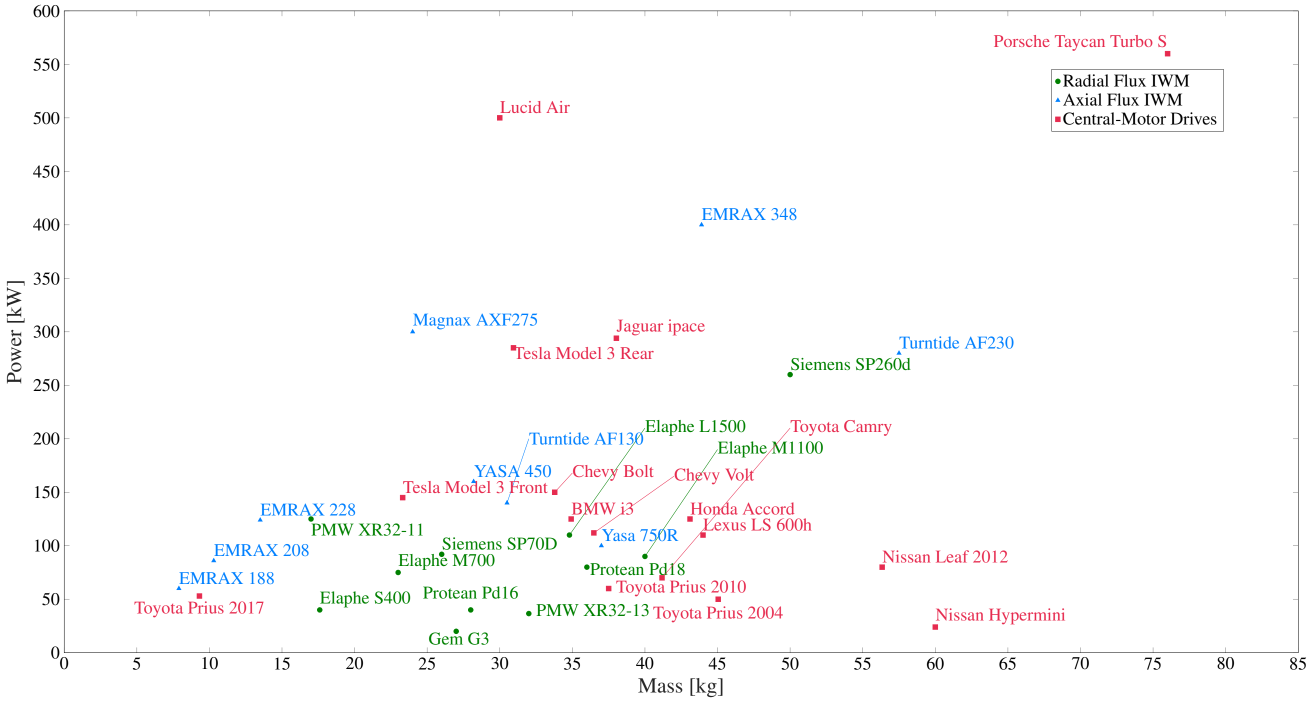

Figure 11. Power vs. mass trend of commercially available radial flux IWM, axial flux IWM, and central-motor drives for EVs.

3. Integrated Power Electronics in IWMs

As a result of their significant potential advantages, machine manufacturers are actively involved in developing and producing IMDs. Substituting inefficient motors, improving power density, reducing losses, and reduced prices when compared to separate motor and drive solutions are among the most important advantages of IMDs. According to [69], over the last decade, technological breakthroughs have resulted in the development of strong electronic components capable of withstanding the extreme environments required by certain techniques of integration. The integrated solution has minimized electromagnetic interference (EMI) and winding voltage surge induced by the surge impedence imbalance between the cables and windings by eliminating individual casings and extensive cable runs [70,71]. The volume of the whole drive can be reduced by 10–20% [72] and system costs by 20–40% [73].

Integration of an IWM with an inverter can reduce long connecting wires and additional housing, resulting in increased power/torque density [74]. According to [75] the latest advancements of wide bandgap semiconductors has improved the power density and ability to withstand higher temperature for elongated time of power electronics modules. Therefore, the integrated motor drive system is extremely appealing for EVs with very demanding electric drive volume, mass, and efficiency criteria. An integrated and modular drive topology is proposed using SSDR yokeless and segmented (YASA) AFPM in [76]. GaN switches are used to reduce the size of the converter. To prevent converter overheating, the stator and power converter components are thermally isolated.

Protean has implemented an integrated motor drive technique for its in-wheel system, as depicted in Figure 12. High fault tolerance is achieved in the Protean IWM system by utilizing four sub-motors and four sub-inverters. Only two DC connections are required for the power supply because the inverter is integrated with the motor. This design reduces the efficiency losses associated with the use of connecting cables between the motor and inverter. Nonetheless, there are concerns to be addressed during the development of integrated motor drives. The drive circuits must be capable of surviving harsh on-road conditions, such as high/low temperatures, dirt, water, and vibration, since they are sealed inside the wheel.

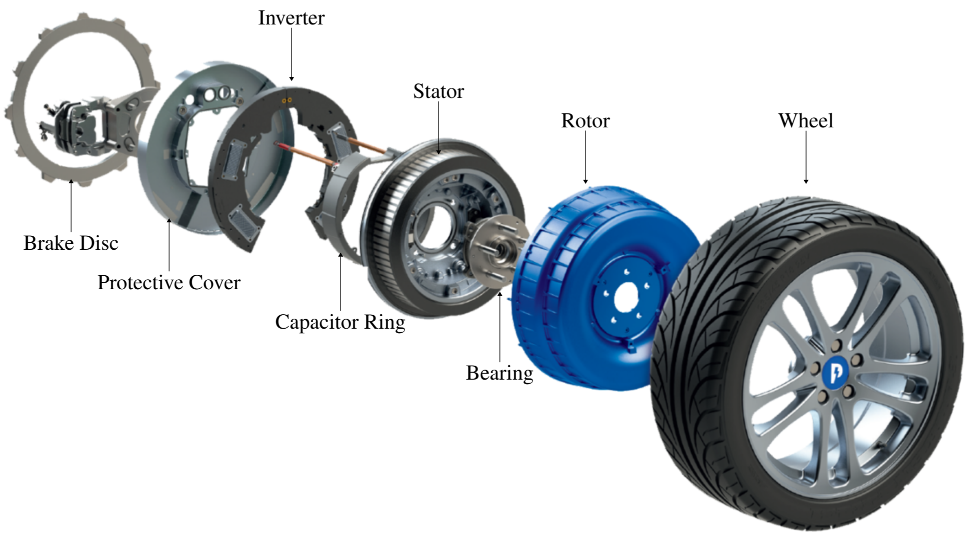

Figure 12. Protean Pd18 exploded view with integrated power electronics [45].

Protean Pd18 and Gem electronics are providing fully integrated power electronics and motor controller in the package. The system efficiency of Gem motors from battery to wheel is between 91–93% and for Protean Pd18 the peak efficiency is 93%.

4. Cooling of IWMs

The IWMs are enclosed within the wheel, making it challenging to dissipate heat when subjected to heavy loads. Hence, it is imperative to equip the IWM with an effective cooling system to guarantee optimal performance and durability. This section discusses the state of the art of cooling methods available for traction motors and applicable to IWM.

4.1. Air Cooling

Air cooling, which is the most fundamental method of cooling motors and is usually used to cool motors with a low heat density, can be accomplished through both natural air cooling on the outer surface and forced air cooling within the motor. A 25 kW air-cooled IMW is proposed in [77] with grooves on the outer surface to increase the cooling surface area exposed to wind. It is concluded that the densely arranged grooves in the same direction as the air flow direction provide the best cooling performance. The study was conducted at a continuous rated operation of 1250 RPM at 40 A and 76.5 N m, and peak performance is not mentioned in the study. [78] designed and verified an air-cooled YASA AFPM motor. To enhance heat dissipation and power density, the novel cooling system utilized aluminum heat-spreading components on each armature section. The heat-spreading components offered a low-resistance heat channel to the surrounding air. GEM Motors also employ natural and forced convection air cooling in their fully integrated IWM as mentioned Table 2.

4.2. Oil Cooling

The oil-cooling method uses a pump to circulate oil as a cooling medium both inside and outside the motor, effectively reducing its temperature. Compared to air, oil has a higher convection coefficient, resulting in superior thermal performance. Additionally, oil can be sprayed directly on the windings for better heat dissipation. To investigate the effect of oil spray cooling on thermal dissipation for higher power output, an oil-cooling system is used for a 35 kW IWM. The cooling path for oil is provided by implementing a hollow shaft cooling channel suitable for IMW [79]. The shape of the oil cooling channel in the hollow shaft is optimized in [80]. The coil temperature in the optimized motor was reported to be reduced by maximum of 13.5 °C. [81] used a multi-objective genetic-algorithm optimization to optimize the cooling channel for oil. In high-torque motors, the current density often exceeds 20 A/mm^2 which results in high copper losses. In general, copper losses account for the highest percentage of losses in the motor. The source of copper is in the winding, hence a direct cooling for the winding can improve the motor efficiency. In [82], an in-slot oil cooling for a PMSM is designed and verified for continuous operation with 25 A/mm^2 and 35 A/mm^2 for 30-s peak operation. Reference [83] reported that with the direct oil cooling for the end winding in AFPM, the oil extracted about 2.8 times more heat compared to the water jacket cooling and effectively double the torque and power density of AFPM as compared to indirect water cooling. However, this method is challenging to implement in outer rotor topology. In [84], a novel winding embedded liquid cooling for slotless motors is proposed. The results showed that proposed method can increase the continuous current density by 35% as compared to in-slot water cooling.

4.3. Water Cooling

The most prominent cooling method for commercial motors, particularly in electric traction applications, is liquid jacket cooling. Heat is expelled by a liquid coolant predominantly by convective heat transfer in the jacket. In most cases, the coolant is water. Glycol is often added to water to decrease the freezing point of the mixture. It is important to use the lowest concentration of glycol necessary to meet the freeze protection requirements because as the concentration of glycol in the solution rises, the effectiveness of the heat transfer fluid drops. The performance of a coolant jacket has been investigated in numerous studies with regard to the channel dimensions, cross-section shape, and flow rate.

A comparison of spiral and axial type cooling water jackets has been investigated in [85]. The authors recommend the use of an axial water jacket due to its higher convective heat transfer coefficient compared to a spiral type water jacket. It should be noted, however, that axial water jackets have a more severe loss in pressure than spiral water jackets for the same amount of heat transfer area [86]. In [87] investigated the effect of flow-rate of the cooling water to optimize the electromagnetic performance of the motor. The thermo-fluid coupling method is used in [88] to analyze the effect of water channel structure parameters on the heat dissipation of the PM in the IWM shown in Figure 13. Based on this analysis, the parameters of the water channel structure are optimized with the suggested chaotic-mapping ant colony algorithm using the metropolis criteria to improve the heat dissipating efficiency of the cooling system. After optimization, an average increase of 23.57% in the convection heat transfer coefficient (CHTC), a reduction in the maximum stator temperature from 95.47 °C to 82.73 °C, and a 14.26% reduction in the peak temperature of the PM are observed. These improvements comprehensively reduce the risk demagnetization in the PM.

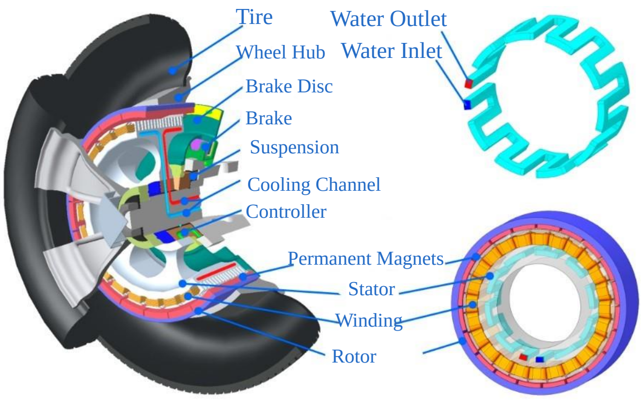

Figure 13. Structure of integrated IWM with cooling jacket [88].

5. Control Methods Used for IWMs and IWM Driven EVs

This section is divided into two parts: firstly, control of the IWM at the component level and later, control methods used in IWM-DEVs to improve the vehicle performance and stability.

5.1. Control of the IWMs

In this section, classic and modern control methods and the motors suitable for control are discussed.

5.1.1. Field Oriented Control (FOC)

FOC is a popular vector-control technique that is commonly used for electric motor drives, particularly for PMSMs [89]. Direct and indirect field-oriented control (DFOC/IFOC) are two approaches to implement FOC for electric motor drives. The main difference between these two methods lies in how the motor current and voltage signals are controlled. In direct FOC, the stator current components in the d-q reference frame are directly controlled by the voltage components in the same reference frame. This is achieved by using a PI controller to regulate the error between the desired and actual stator current and voltage components. Direct FOC is often used in high-performance applications where fast and accurate torque control is required [90]. In contrast, indirect FOC separates the control of the motor's magnetic field and torque by using a separate controller for each component. The magnetic field is controlled indirectly by regulating the stator current in the d-axis, while the torque is controlled by regulating the stator current in the q-axis [91]. Indirect FOC is simpler to implement than direct FOC and is commonly used in low-to-medium performance applications. Direct FOC provides faster and more accurate torque control, but requires more complex algorithms and hardware, while indirect FOC is simpler to implement but may not be as precise in some high-performance applications.

FOC is renowned for its excellent transient response. Figure 14 shows the operating principle of FOC for speed control in PMSM. The principles for FOC are the same whether the PMSM has an inner rotor or outer rotor. FOC for AFPM is implemented using space vector modulation (SVM) technique in [92,93] for both no-load and with load torque conditions.

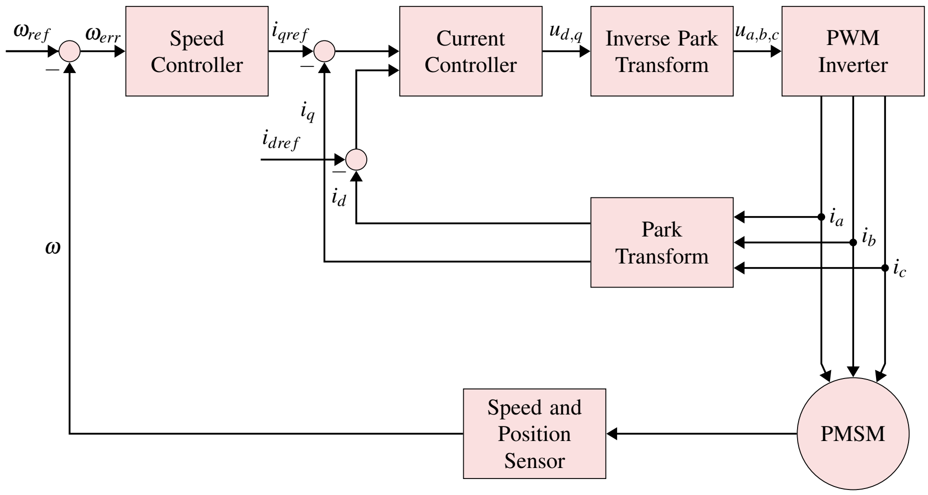

Figure 14. Field oriented control block diagram for speed control in PMSM.

5.1.2. Direct Torque Control (DTC)

DTC is simpler in structure than FOC and works by directly controlling the voltage and frequency applied to the motor based on the desired torque and speed. All calculations are performed in the stator reference frame since precise rotor position information is not required in these systems, except during start-up of the PMSMs. The computational capabilities needed for the controllers are relatively low. These types of systems have superior dynamic features, react promptly to load variations, and are less influenced by alterations in motor properties and interferences. Nevertheless, their steady-state operation has high ripple levels of the stator current, flux linkage, and torque, especially at low speeds, which greatly restricts their usage for high-precision drives [94].

Ref. [95] compares the efficiency and performance of IM used in EVs using two different control methods: IFOC and DTC. The study shows that compared to the IFOC, the DTC approach offers benefits in terms of speed tracking and energy consumption. In [96] the implementation of DTC for controlling AFPM led to a reduction in torque ripples compared to the FOC method.

5.1.3. Model Predictive Control (MPC)

The use of model predictive control (MPC) has become increasingly popular due to advancements in microprocessors, enabling faster and more powerful computing. MPC offers advantages over conventional feedback control schemes, particularly when rapid dynamic response is necessary. It is a versatile control method that can be applied to various systems and is capable of accommodating constraints and non-linearities. MPC is also applicable in multi-variable cases and is easy to implement. Essentially, the MPC method involves using a system model to predict the future behavior of controlled variables, which is then utilized by the controller to determine the optimal actuation based on an optimization criterion.

Predictive control offers the advantage of faster transient responses without the need for a cascaded structure that is usually employed in linear control schemes. However, one major hurdle in using MPC is the necessity for an accurate model, drive parameters, and increased sampling periods due to the large number of computations required.

5.2. Control of Vehicle with IWMs: Torque Vectoring and Torque Distribution

IWM-DEVs offer several advantages, such as an independently controllable four-wheel torque, high energy-utilization rate, and fast motor response speed. The precise control of applied driving and braking torque also enables the use of advanced control methods, such as energy-efficiency control allocation (EECA) algorithms and electric stability control (ESC) based on the coordinated control of driving motors to improve the system performance [97]. However, as an over-actuated system, the control of IWM-DEVs is critical for achieving optimal performance, as the system has more actuators than degrees of freedom. The IWM-DEV's nonlinear dynamics and strong system coupling add to the complexity of the control problem [98].

Disadvantages of independent motor control [98]:

- Non-linearity in the vehicle dynamics due to the coupling of longitudinal, lateral, and yaw dynamics, as well as the non-linear tire longitudinal and lateral characteristics;
- The issue of over-actuation occurs due to the fact that there are four control inputs (torques on four wheels) which exceed the number of states requiring control. As a result, it is necessary to allocate torque based on specified objectives.

To obtain lateral stability control, intensive research has been carried out and two main control methods have been focused on:

- Direct yaw moment control (DYC): DYC uses independent drive motors that are equipped on IWM-DEVs as actuators. By distributing torque in a specific manner, DYC generates a yaw moment that enables the control of vehicle lateral stability [99–101];
- Active front steering (AFS) control: AFS offers an electronically controlled superimposition of an angle to the steering wheel angle, allowing for a continuous and driving-situation dependent adaptation of the steering characteristics. This additional degree of freedom enables the optimization of steering comfort, effort, and dynamics [102–104].

Moreover, there has been research into integrating both DYC and AFC methods for vehicle lateral stability. The authors in [105] developed control methods for this purpose. In [106] proposed an integrated MPC-based approach that uses both AFS and DYC to track the path and improve handling stability. In [107] authors suggested a hierarchical controller for four-wheel independent drive autonomous cars that incorporates an adaptive sliding mode high-level algorithm and a pseudo-inverse control allocation strategy, and assesses immeasurable disturbances through a fuzzy control system. An integrated control architecture is proposed in [108] that combines the MPC and sliding mode control (SMC) to achieve integrated control of AFC and DYC, using a driving state prediction algorithm for online risk assessment.

There is a growing demand for research of the torque distribution control of the entire vehicle, as all wheels can be controlled independently [109]. A review of the design of torque distribution schemes was conducted in [110], using various algorithms such as genetic algorithm, BP neural network, particle swarm algorithm, and fuzzy control algorithm to distribute torque in IWM. The main conclusion drawn from the review was that the future key study areas include the combination of pertinent theoretical research findings and real car test verification under challenging and varied working situations. Additionally, safety and the thorough investigation of energy efficiency must be strengthened in the torque distribution scheme developed in the future.

Extensive research is being conducted to improve the limited driving range of in-wheel motor-driven electric vehicles. Advanced high-energy dense batteries are being developed, while the torque vector control on each wheel is being implemented to reduce motor energy consumption [111–114]. A dual-MPC-based hierarchical control framework has been proposed in [115] to achieve optimum energy consumption and stability control for IWM-

DEV. The upper layer of the framework allocates the torque vector to the front and rear wheel axles to allocate a high-efficiency work zone for IWM. The lower layer deploys a DYC input to provide continuous vehicle handling and cornering stability. Simulation results showed that the proposed controller can reduce energy consumption by 11.29% and 10.81% compared to traditional torque allocation combined linear quadratic regulator controller at a high-speed double-lane-change maneuver and U-turning maneuver, respectively, while ensuring vehicle lateral stability.

The authors in [116] presented the execution of multiobjective optimization design, duty-cycle model predicate current control, and performance verification for an OR-PMSM used in a IWM-DEV. They introduced a state feedback controller that has been fine-tuned and exhibits excellent performance in terms of both tracking and suppressing disturbances. Similarly, by using an optimization method that includes a response surface model and a multi-objective optimization algorithm, the bearingless PMSM design achieves better suspension stability and torque [117]. The optimization method takes into consideration not only the geometrical parameters, but also the winding pattern distribution. Finally, the experimental results confirm the efficacy and the advantage of the optimal design. A novel algorithm is proposed in [118] by improving the nondominated sorted genetic algorithm III to reduce the optimization time while optimizing the IWM to achieve higher torque and lower torque ripple. The experimental results verified the results obtained by FEA. Hence, by applying various multi-objective optimization methods for IWM motor and its various parameters, such as winding pattern distribution, driving cycle based efficiency, and thermal design, the vehicle performance can be improved.

6. Mechanical Failures and Challenges in IWMs Driven EVs

IWM-DEVs reduce the need for reduction gears and differential gear, hence, the mechanical losses in the power transmission are reduced. Moreover, the extra space in the chassis can be used for bigger battery systems, hence longer mileage.

There is abundance of literature about the electromagnetic optimization, electric faults and failures of IWM. This section presents the drawbacks and issues in IWM with mechanical origin. The optimal performance of an in-wheel motor requires optimization of the mechanical design, including the housing elements, thermal management, dimensional tolerances, and selection of appropriate hub bearings, to ensure consistent electromagnetic properties. Most of the critical mechanical drawbacks and failures are enlisted below:

- Increased unsprung mass results in poorer vehicle dynamics;
- Thermomechanical influences, caused by the variation in expansion of the materials in an assembly, which results in a subsequent stress-strain state;
- Sudden and unanticipated external impacts can cause the structural elasticity to become distorted;
- The effect of torque pulsation-related vibrations on acoustics and structural fatigue;
- Bearing system faults leading to mechanical breakdowns.;
- Static or dynamic eccentricity induced mechanical defects;
- Challenges for sealing of IWM.

These faults are directed to the IWMs effect on driving dynamics, mechanical constructions and motor failures. The following subsections describe the nature of the failures, their cause, and their effect on the IWM driving system. In [14], the authors explore the relationship between the desired electromagnetic parameters and necessary geometrical constraints to guarantee an efficient and high-performing operation.

6.1. Unsprung Mass

The unsprung mass is the most quoted drawback of the IWM in both academic and industrial research papers [119]. This study analyzed the impact of IWM on a vehicle's performance, and it was found that increased unsprung mass has a noticeable but not severe impact on active safety and driveability. The study also found that there is no discernible difference in the primary ride on smooth roads, and only a slight degradation in rough road performance, while a secondary ride may require changes to seat or suspension components. Restoring agility may require slight modifications to the suspension components.

The authors in [120] proposed a combined structure consisting of a controlled suspension and a controlled tuned mass damper (TMD) to eliminate the unsprung adverse effect of IWM-DEVs. Designing a sliding mode controller for both the suspension and the TMD is an effective method for improving ride comfort and suppressing vibrations, as demonstrated by the suggested method, which showed better response in vibration management and led to improved ride comfort and road-holding. The study in [121] analyzed the effects of IWM on vehicle stability, safety, and ride comfort based on a quarter vehicle suspension model. During simulations, the occurrence of wheel hop, which is dependent on unsprung mass and tire stiffness, was monitored. The results showed potential handling problems at higher velocities, but the researchers concluded that traditional suspension of a passenger car could be used for IWM-DEVs without compromising comfort and safety. On the other hand, IWMs exhibited wheel hop, leading to a longer time required for the tire to regain contact with the surface.

6.2. Vibrations Sources

The growing demand for improved NVH (noise, vibration, and harshness) performance in EVs has led to increased research on the causes and mitigation of vibrations in these vehicles. However, the placement of motors in EVs with IWM drive systems is different from those with central-motor drive systems. Therefore, there is a need for special attention to investigate additional vibration causes and their effects in EVs with in-wheel drive systems.

Ref. [122] categorized the IWM vibrations as vibrations induced by internal sources and vibrations induced by external sources. The internally induced vibrations are caused by the electromagnetic coupling, which are further subdivided as electromagnetic vibration, mechanical vibration, and aerodynamic vibration. Figure 15 shows a typical flowchart to simulate and analyze the vibrations caused by electromagnetic forces in a motor using FEA. Electromagnetic vibration is recognized as the most significant element among these categories and eccentricity is the main source of electromagnetic vibrations. Eccentricity can be static or dynamic, with the latter being caused by worn bearings, curved shafts, or high levels of static eccentricity. Static eccentricity arises when the rotor is not positioned at the magnetic center of the stator, resulting in an uneven air gap. Dynamic eccentricity is a condition where the position of the minimum radial air gap rotates with the rotor. Eccentricity generates an unbalanced electromagnetic force (UEMF), which causes the motor structure and the motor to vibrate. Abnormal rotation, mass imbalance, and external forces can induce rotor eccentricity, further increasing UEMF and altering air-gap distribution, forming a typical electromechanical coupling system.

The machine-cooling systems (air, water, or oil cooling) are the principal sources of aerodynamic vibration in all motors. The failures caused by eccentricity are discussed in next section.

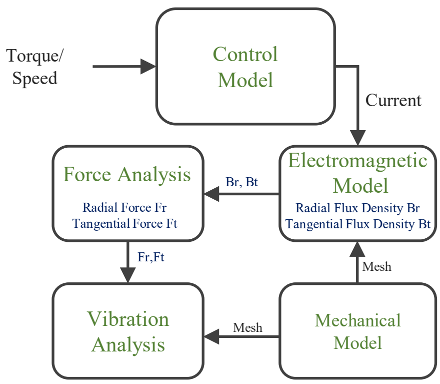

Figure 15. Flowchart of electromagnetic forces and vibration calculations with FEA [122].

6.3. Eccentricity

In [123] the authors discuss the impact of electromechanical coupling between electromagnetic excitation in the motor, and transient dynamics in the vehicle is established and developed. Eccentricity is developed because of the unbalanced magnetic forces and the eccentricity has a negative impact on the vertical dynamics of the vehicle.

Figure 16 shows the effect of eccentricity on the airgap deformation. Figure 17 explains the logical diagram used to reduce the eccentricity based faults in IWM.

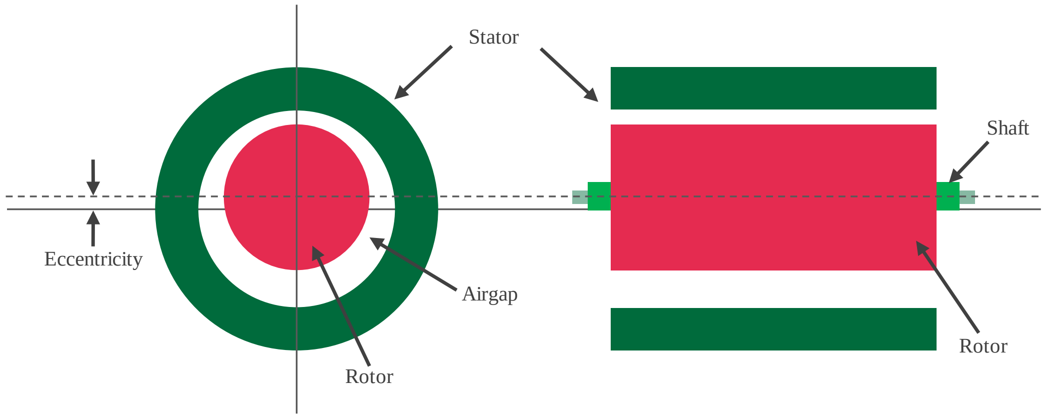

Figure 16. Airgap deformation due to eccentricity [123].

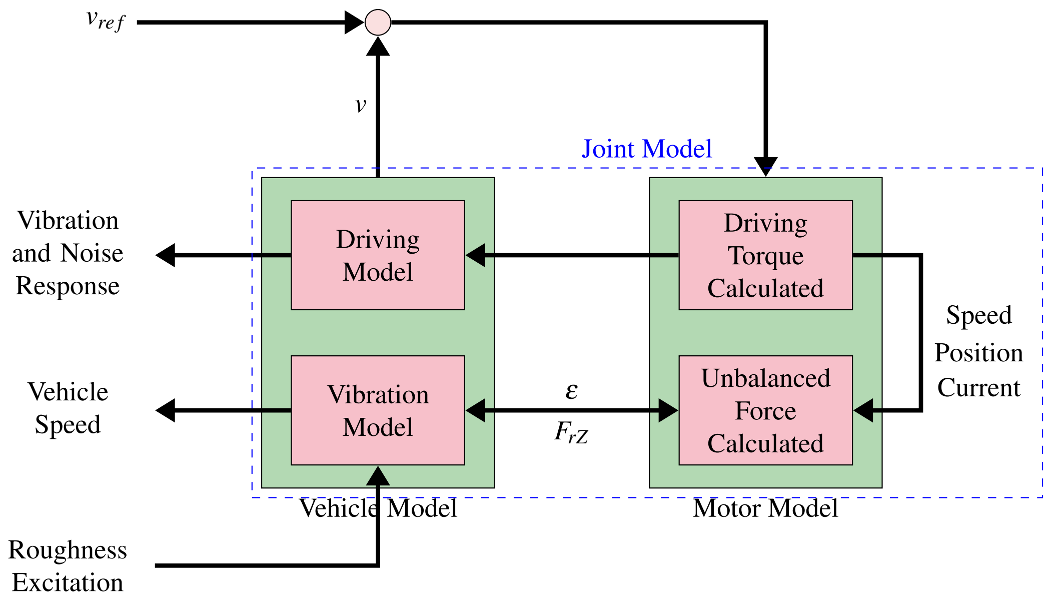

Figure 17. Electro-mechanical coupling model developed to reduce the eccentricity based faults in IWM [123].

Ref. [124] stated that studies on the vibration characteristics of electric vehicles with IWM have typically ignored the impact of transmission components such as the motor and bearing. Instead, they focus on the dynamic performance of the vehicle while driving on a road surface. However, recent research indicates that rotor-bearing coupling vibration can significantly affect the vehicle's dynamic behavior, particularly in terms of tire vibration acceleration and dynamic load. Ref. [121] analyzed the impact of an in-wheel motor (IWM) suspension system on the ride comfort of electric vehicles (EVs) by considering various road surface roughness and IWM mass conditions. The study found that the IWM suspension system significantly improved EV ride quality, reducing the weighted root-mean-square acceleration of the vertical vehicle body by 8.6% compared to without the IWM suspension system. The study also highlighted the importance of considering the impact of transmission components such as the motor rotor and bearing on EV dynamic performance. While previous research has focused on the impact of motor exciting force, the influence of rotor-bearing coupling vibration on EV dynamic performance requires further study.

6.4. Bearing Faults

Hub bearings are recognized as a critical component for IWM application in various studies, such as [125–128]. These studies analyze acting loads and their effects on component deformation, using analytically and numerically determined stiffness, and validated through measurements at the component and assembly level to ensure functionality under a wide range of operations. The stiffness properties of the bearing have been found to have a significant impact on performance optimization. Therefore, it is crucial to optimize the stiffness properties, package size, and weight for a specific application [129].

6.5. Sealing

Although they lack glamour, seals and sealant materials are indispensable in contemporary vehicles, as they serve to prevent contaminants from entering and fluids from leaking out of the vast majority of systems and components. The seals are composed of specially formulated polymer compounds that must endure extreme temperatures, vibrations, dust, fluid exposure, and chemical corrosion over long periods of use and tens of thousands of miles. Furthermore, they must be easily applicable during manufacturing and conform to health, safety, and environmental regulations. Reference [130] mentioned a design approach for motor requirements and safety standards, specifically for external rotor motors. The approach includes increasing the diameter of seals to handle the higher braking torque generated by the larger diameter of the motor. However, this approach has a drawback as it allows the ingress of water and particles into the motor unit, which can damage the windings and electronics components, compromising the lifetime of subcomponents. This problem is solved by a new sealing method with a breather that allows moisture to escape, called the V seal. The main V seal is the outermost seal, also allowing a high-pressure jet wash. A sealing method specific for the wheel hub motor is presented and patented in [131].

7. Next Trends

7.1. Magnet Price Crisis and Rare Earth Magnets Availability

In the present market for permanent magnets, four major types of magnets are available based on the material used to manufacture them, namely:

1. Ferrite magnets;
2. Alnico magnets;
3. Neodymium magnets;
4. Samarium cobalt magnets.

The ferrite permanent magnets are also known as ceramic magnets because they are electrically insulating. Their typical composition consists of large proportions of iron oxide blended with elements such as strontium, manganese, nickel, barium, and zinc. Similar to many other ceramics, ferrites are characterized by their hardness and brittleness. With regards to their magnetic characteristics, ferrites are commonly categorized as either "soft" or "hard", referring to their low or high magnetic coercivity, respectively.

Consisting of a combination of aluminum, nickel, and cobalt, Alnico magnets provide a strong magnetic field and possess low coercivities, while exhibiting greater durability than rare earth magnets. They also exhibit exceptional resistance to corrosion, remain stable under varying temperatures, and can endure extremely high temperatures (with maximum operating temperatures up to 550 °C). They can be produced in intricate shapes, such as horseshoe shapes, which are unattainable with alternative magnetic materials, through either casting or sintering techniques.

Neodymium and samarium cobalt magnets are collectively called rare earth magnets. These magnets are currently the most powerful permanent magnets available commercially, outperforming ferrite (ceramic) and alnico magnets by a wide margin. Although the label "rare earth" may seem to imply scarcity, rare earth metals are actually fairly abundant within the Earth's crust. However, the process of mining these metals is often economically challenging, as they are usually mixed with other elements and not typically found in concentrated form. The primary composition of neodymium magnets consists of neodymium, boron, and iron, while small amounts of elements such as praseodymium (Pr), dysprosium (Dy), aluminum (Al), and niobium (Nb) are added to improve their properties, including strength, temperature resistance, and demagnetization and corrosion resistivity. Similarly, samarium cobalt consists primarily of samarium and cobalt with small amounts of praseodymium (Pr), zirconium (Zr), hafnium (Hf), iron (Fe), and copper (Cu).

Permanent magnets are compared based on the following properties:

- Remanence, B_r: measures the strength of the magnetic field;
- Coercivity, H_c: is the resistance of the material to being demagnetized;
- Maximum energy product (BHmax): is the density of magnetic energy is determined by the product of the maximum value of magnetic flux density (B) and magnetic field strength (H);
- Curie temperature: the temperature at which the material loses its magnetism completely;
- Maximum operating temperature: the normal operating range of magnet; below this temperature demagnetization is reversible.

Figure 18 shows a comparison between the maximum energy product and maximum operating temperature of PMs based on their manufacturing material [132]. The data clearly indicates that sintered NdFeB PMs are the strongest PMs available, but they have a restricted maximum operating temperature. Conversely, Alnico is the most resilient to high operating temperatures, but its maximum energy product is nearly ten times weaker than that of NdFeB PMs.

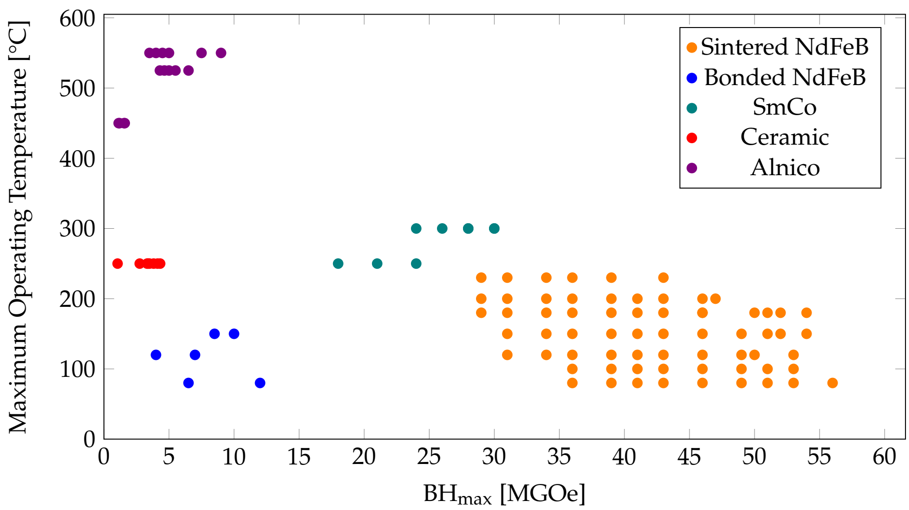

Figure 18. Different grade of magnets BHmax and maximum operating temperature [132].

Serious concerns about the future supply of rare earth minerals have arisen due to China's dominant position as a producer of over 95 percent of the world's output and its decision to restrict exports. In addition, the rapid growth in the consumption of rare earth, particularly for new clean energy technologies such as electric mobility, has exacerbated these concerns. Figure 19 shows the countries that produce the most RE elements. Concerns have also been raised about the lack of transparency in the supply chain and the environmental, social, and governance issues associated with the mining and production of rare earths. As a result, industrial countries such as Japan, the United States, and countries in the European Union are experiencing shortages and increased prices for these essential materials. It is worth noting that rare earths are critical to the European EV economy. Over 95% of EVs [133] use RE PM traction motors owing to their high torque density they provide. Therefore, an alternative to RE based traction motors is highly sought after in the EU EV market [134].

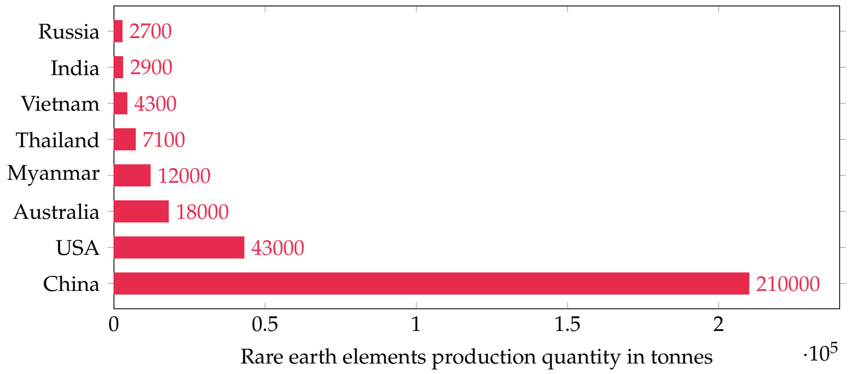

Figure 19. Countries with most rare earth metals production in 2022 [135].

7.2. Alternatives to RE Based IWMs

The IWM which utilizes RE magnets has shown promise due to its high torque density and efficiency. However, the continuously growing spike prices of RE materials has led to the need for the development of electric motors that do not rely on RE magnets. Several non-PM machines such as OM-IM, OR-SRM, and OR-SynRM have been reviewed in this paper for use in IWM drive systems. However, the torque densities of these non-PM machines are not comparable to that of PMSM.The use of RE free magnets, such as ceramic/ferrite or AlNiCo, may lead to potential demagnetization under heavy loads. Therefore, the development of high torque density electrical machines that rely on fewer or no rare earth magnets is still a challenge, but one that must be addressed if PMSM is to be replaced in in-wheel drive EVs. The EU project ReFreeDrive [136] is focused on reducing the reliance on rare earth magnets by developing a new generation of electric driven trains that are both industrially viable for large-scale production and cost-effective in terms of manufacturing technologies. However this project developed IM and SynRM (both internal rotors) suited for central drive EVs. There is a need for such initiatives to develop RE free motors specifically for IWM applications.

7.3. Wireless IWMs

A conceptual IWM with wireless technology is shown in the review of IWM. In [137], a novel wireless IWMs is introduced. The transmission cables between the IWM and the battery is replaced by the wireless power transfer (WPT) technology. Figure 20 shows the working principle of the wireless IWM using a WPT.

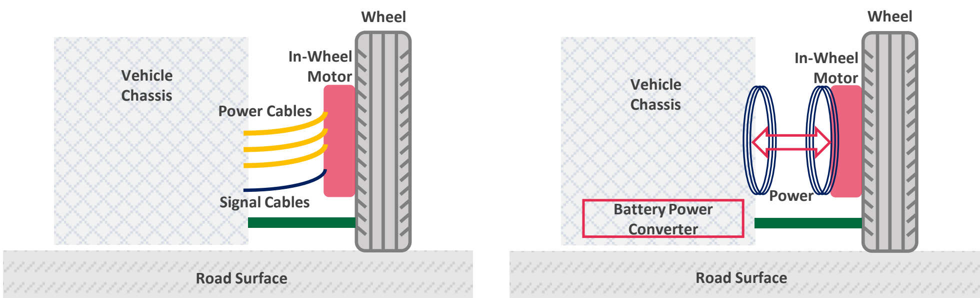

(**a**) Conventional IWM (**b**) Wireless IWM

Figure 20. Magnetic flux is produced (**a**) radially along the rotor in RFM (**b**) axially along the axis of rotor in AFM.

7.4. Field-Modulated Motors for IWM Driven EVs

Field-modulated motors have unique characteristics that distinguish them from conventional synchronous motors. One such feature is that the pole-pair number of the stator may differ from that of the rotor, which is contrary to the basic rule for conventional motor design that requires the number of pole pairs of the stator and the rotor to be the same [138]. Flux-switching motors, magnetic gear motors, vernier motors, and motors with dual rotor or stators all fall under the category of field-modulated motors. These motors have been researched and utilized recently for IWM applications as well because of their ability to provide a higher torque for same number of pole-pairs as compared to a conventional PMSM.

A magnetically geared motor (MGM) is an electric motor that utilizes a magnetic gear to transmit torque to the load. The MGM, as shown in Figure 21, is a compound machine which is composed of a PMSM installed in the inner part and a magnetic gear installed in the outer part. The outer rotor of the PMSM is connected to the inner rotor of the magnetic gear, which consists of two rotors with magnetic poles facing each other. However, there is no physical contact between the rotors, and the torque is transmitted through the interaction between the magnetic fields of the rotors. The outer rotor of the magnetic gear can be connected directly to the wheel, making it suitable for IWM applications [139–143].

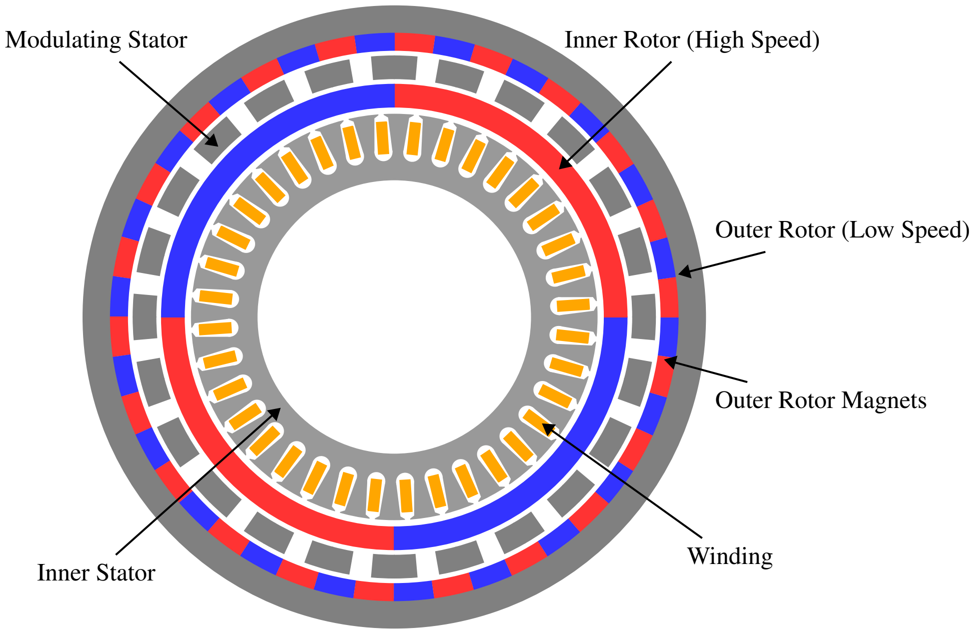

Figure 21. Topology of a magnetically gear motor [144].

The vernier PM motor (VPM) uniquely utilizes an additional modulation flux due to the magnetic modulation effects in addition to the regular PM flux. Due to these effects, the VPMs produce much higher back EMF and higher power density than conventional PMSMs [145]. The special shape of the stator, as shown in Figure 22, causes the modulation effect to happen. Like PMSM motors, vernier motors also typically have inner-rotor topologies and have similar disadvantages, such as long end-windings and the inefficient use of motor inner space, and to overcome these two advantages [146] proposed an outer-rotor VPM using toroidal winding. A quantitative comparison among inner-rotor VPM (IR-VPM), outer-rotor VPM (OR-VPM), and outer-rotor consequent pole VPM (OR-CP-VPM) has been carried out in [147]. It is concluded that by employing toroidal winding and outer rotor topology, the motors achieve higher efficiencies and torque density. The major disadvantages are high PM flux leakage and manufacturing complexity. An OR-VPM with an open-slot stator is proposed in [148] to reduce the iron in the stator, consequently increasing the efficiency. A comparison of in-wheel VPM with sintered and bonded NdFeB magnets is performed in [149], showing that low-performance bonded NdFeB magnets are sufficient to provide the specified IWM required as compared to sintered NdFeb PM, which have higher processing costs. Reference [150] proposed a VPM with flux barriers to reduce the first-order harmonic to reduce the rotor losses while maintaining the torque density. The test results concluded that first harmonic only affect the rotor losses and no effect on average torque. In [151], a (OR-CP-VPM) for IWM applications is proposed. A consequent pole rotor has same polarity of magnets in the rotor as compared to conventional rotors where polarity is alternating. Using consequent pole and toroidal winding improved the torque and back EMF by ∼20% and ∼34% less than the magnets' consumption.

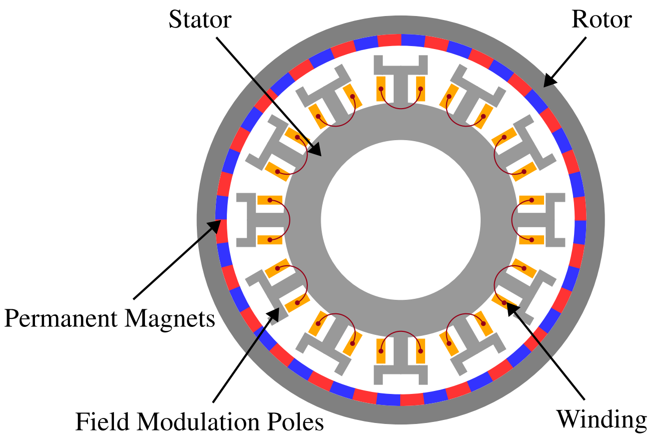

Figure 22. Topology of an outer-rotor vernier permanent-magnet motor [152].

8. Conclusions

To make effective use of IWMs in EVs, it is essential to design motors that are both power and torque dense and which can withstand the harsh conditions present in the wheel, including thermal isolation and vibration. In-wheel motor drive systems are more desirable than traditional central-drive systems since they eliminate mechanical transmission components, leading to reduced noise and vibration, lower maintenance costs, increased transmission efficiency, and greater flexibility in vehicle wheel control.

The conventional SM-OR-PMSM and AF-PMSMs are attractive choices for IWM-DEV due to their compact structure and high torque density, and they are currently being used in the industrial IWM sector. In order to achieve a more compact IWM drive, integrated motor drives that include the power inverter and cooling solution are being explored. As an alternative to PM machines, the cost-effective OR-SRM, OR-SynRM, and OR-IM have been considered, but their torque densities are significantly lower than PM-equipped motors. The recently developing field-modulated motors have satisfactory torque density, but their motor topology is complex, and their power factor is comparatively small, which limits their real-world applications in the industry.

The utilization of torque distribution techniques in electric vehicles with in-wheel motors is in high demand as it can improve the system's energy efficiency and enhance vehicle stability. In addition, there is a need for lighter motors with high torque to reduce unsprung mass, along with advanced suspension systems to provide a smoother and more comfortable ride for in-wheel motor drive electric vehicles. The current rare-earth material crisis requires the development of alternative motors that are free of permanent magnets or rare-earth materials.

Author Contributions: Writing—first draft and review, K.D.; writing—review and editing, M.A.F., Y.B., and M.E.B., supervision, O.H. All authors have read and agreed to the published version of the manuscript.

Funding: This study was funded by a Vrije Universiteit Brussel (VUB) scholarship.

Data Availability Statement: Not applicable.

Acknowledgments: The authors acknowledge the support of Flanders Make for our research group.

Conflicts of Interest: The authors declare no conflict of interest.

Abbreviations

The following abbreviations are used in this paper:

AFM	Axial Flux Motor
AFIM	Axial Flux Induction Motor
AFPM	Axial Flux Permanent Magnet Motor
AF-SRM	Axial Flux Switched Reluctance Motor
BEV	Battery Electric Vehicle
CP	Consequent Pole
DTC	Direct Torque Control
DSSR	Double Stator Single Rotor
EU	European Union
EV	Electric Vehicle
FEA	Finite Element Analysis
FOC	Field Oriented Control
HEV	Hybrid Electric Vehicle
ICE	Internal Combustion Engine
IM	Induction Motor
IPMSM	Internal Permanent Magnet Synchronous Motor
IWM	In-Wheel Motor
IWM-DEV	In-Wheel Motor Driven Electric Vehicle
OR-IM	Outer Rotor Induction Motor
OR-PMSM	Outer Rotor Permanent Magnet Synchronous Motor
MGM	Magnetically Geared Motor
MGOe	Mega Gauss Oersted
MPC	Model Predictive Control
MSMR	Multi Stator Multi Rotor
NdFeB	Neodymium Iron Boron
NVH	Noise, Vibration and Harshness
PM	Permanent Magnet
PMSM	Permanent Magnet Synchronous Motor
RE	Rare Earth
RFM	Radial Flux Motor
SmCo	Samarium Cobalt
SSSR	Single Stator Single Rotor
SSDR	Single Stator Double Rotor
SVM	Space Vector Modulation
SRM	Switched Reluctance Motor
SynRM	Synchronous Reluctance Motor
TMD	Tuned Mass Damper
VPM	Vernier Permanent Magnet Motor
WPT	Wireless Power Transfer

References

1. Hawkins, T.R.; Gausen, O.M.; Strømman, A.H. Environmental impacts of hybrid and electric vehicles—A review. *Int. J. Life Cycle Assess.* **2012**, *17*, 997–1014. [CrossRef]
2. Pg Abas, A.E.; Yong, J.; Mahlia, T.M.; Hannan, M.A. Techno-economic analysis and environmental impact of electric vehicle. *IEEE Access* **2019**, *7*, 98565–98578. [CrossRef]
3. Albatayneh, A.; Assaf, M.N.; Alterman, D.; Jaradat, M. Comparison of the Overall Energy Efficiency for Internal Combustion Engine Vehicles and Electric Vehicles. *Environ. Clim. Technol.* **2020**, *24*, 669–680. [CrossRef]
4. Krings, A.; Monissen, C. Review and trends in electric traction motors for battery electric and hybrid vehicles. In Proceedings of the 2020 International Conference on Electrical Machines, ICEM 2020, Gothenburg, Sweden, 23–26 August 2020; pp. 1807–1813. [CrossRef]

5. Hecht, C.; Spreuer, K.G.; Figgener, J.; Sauer, D.U. Market Review and Technical Properties of Electric Vehicles in Germany. *Vehicles* **2022**, *4*, 903–916. [CrossRef]
6. Burress, T.A.; Campbell, S.L.; Coomer, C.; Ayers, C.W.; Wereszczak, A.A.; Cunningham, J.P.; Marlino, L.D.; Seiber, L.E.; Lin, H.T. *Evaluation of the 2010 Toyota Prius Hybrid Synergy Drive System*; Technical Report; Oak Ridge National Lab: Oak Rigde, TN, USA, 2011. [CrossRef]
7. Wellings, J.; Greenwood, D.; Coles, S.R. Understanding the Future Impacts of Electric Vehicles—An Analysis of Multiple Factors That Influence the Market. *Vehicles* **2021**, *3*, 851–871. [CrossRef]
8. Sanguesa, J.A.; Torres-Sanz, V.; Garrido, P.; Martinez, F.J.; Marquez-Barja, J.M. A Review on Electric Vehicles: Technologies and Challenges. *Smart Cities* **2021**, *4*, 372–404. [CrossRef]
9. Mierlo, J.V.; Berecibar, M.; Baghdadi, M.E.; De Cauwer, C.; Messagie, M.; Coosemans, T.; Jacobs, V.A.; Hegazy, O. Beyond the State of the Art of Electric Vehicles: A Fact-Based Paper of the Current and Prospective Electric Vehicle Technologies. *World Electr. Veh. J.* **2021**, *12*, 20. [CrossRef]
10. Yong, J.Y.; Ramachandaramurthy, V.K.; Tan, K.M.; Mithulananthan, N. A review on the state-of-the-art technologies of electric vehicle, its impacts and prospects. *Renew. Sustain. Energy Rev.* **2015**, *49*, 365–385. [CrossRef]
11. Zhao, Y.; Zhang, Y.; Zhao, Y. Stability control system for four-in-wheel-motor drive electric vehicle. In Proceedings of the 6th International Conference on Fuzzy Systems and Knowledge Discovery, FSKD 2009, Tianjin, China, 14–16 August 2009; Volume 4, pp. 171–175. [CrossRef]
12. The History of Porsche Begins Electrically—Porsche Newsroom. Available online: https://newsroom.porsche.com/en/products/taycan/history-18563.html (accessed on 21 February 2023).
13. 1900 Lohner-Porsche Mixte Voiturette—Images, Specifications and Information. Available online: https://www.ultimatecarpage.com/car/3456/Lohner-Porsche-Mixte-Voiturette.html (accessed on 24 February 2023).
14. Biček, M.; Gotovac, G.; Miljavec, D.; Zupan, S. Mechanical Failure Mode Causes of In-Wheel Motors. *Stroj. Vestn. J. Mech. Eng.* **2015**, *61*, 74–85. [CrossRef]
15. Cai, S.; Kirtley, J.L.; Lee, C.H. Critical Review of Direct-Drive Electrical Machine Systems for Electric and Hybrid Electric Vehicles. *IEEE Trans. Energy Convers.* **2022**, *37*, 2657–2668. [CrossRef]
16. Aloeyi, E.F.; Ali, N.; Wang, Q. A Review of In-Wheel Motors for Electric Vehicle Propulsion. In Proceedings of the 2022 IEEE Transportation Electrification Conference and Expo, Asia-Pacific (ITEC Asia-Pacific), Haining, China, 28–31 October 2022; pp. 1–6. [CrossRef]
17. Gong, J.; Zhao, B.; Huang, Y.; Semail, E.; Nguyen, N.K. Quantitative Comparisons of Outer-Rotor Permanent Magnet Machines of Different Structures/Phases for In-Wheel Electrical Vehicle Application. *Energies* **2022**, *15*, 6688. [CrossRef]
18. Xue, X.D.; Cheng, K.W.; Ng, T.W.; Cheung, N.C. Multi-objective optimization design of in-wheel switched reluctance motors in electric vehicles. *IEEE Trans. Ind. Electron.* **2010**, *57*, 2980–2987. [CrossRef]
19. Lucid Motors Tech Talk On Drive Unit & Motor—Lucid Insider Blog—Lucid Air & Lucid Motors News. Available online: https://www.lucidinsider.com/2022/09/13/lucid-motors-tech-talk-on-drive-unit-motor/ (accessed on 23 February 2023).
20. Goli, C.S.; Manjrekar, M.; Essakiappan, S.; Sahu, P.; Shah, N. Landscaping and review of traction motors for electric vehicle applications. In Proceedings of the 2021 IEEE Transportation Electrification Conference and Expo, ITEC 2021, Chicago, IL, USA, 23–25 June 2021; pp. 162–168. [CrossRef]
21. Porsche Taycan Finally Revealed. Available online: https://www.electrive.com/2019/09/04/porsche-taycan-finally-revealed/ (accessed on 23 February 2023).
22. Wang, X.; Zhang, Z.; Gao, P.; Lu, H.; He, X. Design and Simulation Analysis of a Novel Outer Rotor IPM Motor Used in Electric Vehicles. In Proceedings of the 13th World Congress on Intelligent Control and Automation (WCICA), Changsha, China, 4–8 July 2018.
23. Fan, Y.; Chen, S.; Tan, C.; Cheng, M. Design and investigation of a new outer-rotor IPM motor for EV and HEV in-wheel propulsion. In Proceedings of the 19th International Conference on Electrical Machines and Systems (ICEMS), Chiba, Japan, 13–16 November 2016.
24. Ishii, S.; Hasegawa, Y.; Nakamura, K.; Ichinokura, O. Characteristics of Novel Flux Barrier Type Outer Rotor IPM Motor with Rare-earth and Ferrite Magnets. In Proceedings of the 2012 International Conference on Renewable Energy Research and Applications (ICRERA), Nagasaki, Japan, 11–14 November 2012. [CrossRef]
25. Fornasiero, E.; Morandin, M.; Carraro, E.; Bianchi, N.; Bolognani, S. Outer Rotor IPM Generator with Wide Constant Power Region for Automotive Applications. In Proceedings of the 2014 IEEE Transportation Electrification Conference and Expo (ITEC), Dearborn, MI, USA, 15–18 June 2014. [CrossRef]
26. Yao, Y.; Liu, C.; Lee, C.H. Quantitative comparisons of six-phase outer-rotor permanent-magnet brushless machines for electric vehicles. *Energies* **2018**, *11*, 2141. [CrossRef]
27. Labak, A.; Kar, N.C. Outer rotor switched reluctance motor design for in-wheel drive of electric bus applications. In Proceedings of the 2012 20th International Conference on Electrical Machines, ICEM 2012, Marseille, France, 2–5 September 2012; pp. 418–423. [CrossRef]
28. Yaling, W.; Yanliang, X.; Yufang, W.; Yun, Z. Outer-rotor switched reluctance motor and its control system used in electric vehicles. In Proceedings of the 2011 International Conference on Electrical Machines and Systems, ICEMS 2011, Beijing, China, 20–23 August 2011. [CrossRef]

29. Boldea, I.; Tutelea, L.N.; Parsa, L.; Dorrell, D. Automotive electric propulsion systems with reduced or no permanent magnets: An overview. *IEEE Trans. Ind. Electron.* **2014**, *61*, 5696–5711. [CrossRef]
30. Zhu, J.; Cheng, K.W.E.; Xue, X.; Zou, Y. Design of a New Enhanced Torque In-Wheel Switched Reluctance Motor with Divided Teeth for Electric Vehicles. *IEEE Trans. Magn.* **2017**, *53*, 2703849. [CrossRef]
31. Qin, Y.; He, C.; Shao, X.; Du, H.; Xiang, C.; Dong, M. Vibration mitigation for in-wheel switched reluctance motor driven electric vehicle with dynamic vibration absorbing structures. *J. Sound Vib.* **2018**, *419*, 249–267. [CrossRef]
32. Zhu, Y.; Zhao, C.; Zhang, J.; Gong, Z. Vibration control for electric vehicles with in-wheel switched reluctance motor drive system. *IEEE Access* **2020**, *8*, 7205–7216. [CrossRef]
33. Jurca, F.N.; Martis, C. Analysis of outer rotor synchronous reluctance motor for low-speed applications. In Proceedings of the International Conference on Electical Drives and Power Electronics, Dubrovnik, Croatia, 4–6 October 2017; pp. 242–247. [CrossRef]
34. Aghazadeh, H.; Afjei, E.; Siadatan, A. Sizing and detailed design procedure of external rotor synchronous reluctance machine. *IET Electr. Power Appl.* **2019**, *13*, 1105–1113. [CrossRef]
35. Bozkurt, A.; Baba, A.F.; Oner, Y. Design of Outer-Rotor Permanent-Magnet-Assisted Synchronous Reluctance Motor for Electric Vehicles. *Energies* **2021**, *14*, 3739. [CrossRef]
36. Al-ani, M. Multi-physics design and analyses of dual rotor synchronous reluctance machine. *eTransportation* **2021**, *8*, 100113. [CrossRef]
37. Klima, P.; Rura, D.; Vitek, O. Analysis and Reduction of Eddy Current Losses in High-Speed Solid Outer Rotor Induction Machine. In Proceedings of the 2022 International Conference on Electrical Machines, ICEM 2022, Valencia, Spain, 5–8 September 2022; pp. 1022–1026. [CrossRef]
38. Cha, H.R.; Jeong, T.W.; Im, D.Y.; Shin, K.J. Design of outer rotor type induction motor having high power density for in-wheel system. In Proceedings of the 15th International Conference on Electrical Machines and Systems (ICEMS), Sapporo, Japan, 21–24 October 2012.
39. Abdo, T.M.; Adly, A.A. The Outer Solid Rotor Induction Motor as an Alternative for Electric Vehicle Traction Applications. In Proceedings of the 2022 Joint MMM-Intermag Conference, INTERMAG 2022, New Orleans, LA, USA, 10–14 January 2022. [CrossRef]
40. Virlan, B.; Benelghali, S.; Simion, A.; Livadaru, L.; Outbib, R.; Munteanu, A. Induction motor with outer rotor and ring stator winding for Multispeed applications. *IEEE Trans. Energy Convers.* **2013**, *28*, 999–1007. [CrossRef]
41. Rezazadeh, G.; Tahami, F.; Capolino, G.A.; Nasiri-Gheidari, Z.; Henao, H.; Sahebazamani, M. Improved Design of an Outer Rotor Six-Phase Induction Motor With Variable Turn Pseudo-Concentrated Windings. *IEEE Trans. Energy Convers.* **2022**, *37*, 1020–1029. [CrossRef]
42. Virlan, B.; Benelghali, S.; Munteanu, A.; Simion, A.; Outbib, R. Multi-speed induction motor for direct drive applications. In Proceedings of the 2012 20th International Conference on Electrical Machines, ICEM 2012, Marseille, France, 2–5 September 2012; pp. 1928–1934. [CrossRef]
43. Livadaru, L.; Munteanu, A.; Simion, A.; Cantemir, C.G. Design and finite element analysis of high-density torque induction motor for traction applications. In Proceedings of the 2015 9th International Symposium on Advanced Topics in Electrical Engineering, ATEE 2015, Bucharest, Romania, 7–9 May 2015; pp. 211–214. [CrossRef]
44. Virlan, B.; Simion, A.; Livadaru, L.; Benelghali, S.; Outbib, R. Analysis of a three phase induction motor with outer rotor for multi-speed applications. In Proceedings of the 2012 20th International Conference on Electrical Machines, ICEM 2012, Marseille, France, 2–5 September 2012; pp. 411–417. [CrossRef]
45. Technology—ProteanDrive. Available online: https://www.proteanelectric.com/technology/#overview (accessed on 10 February 2023).
46. Elaphe Direct-Drive in-Wheel Motors. Available online: https://in-wheel.com/en/solutions-2/direct-drive-in-wheel-motors/ (accessed on 9 February 2023).
47. PMW Dynamics In-Wheel XR Series Motors. Available online: https://www.pmwdynamics.com/in-wheel-motors/ (accessed on 10 February 2023).
48. GEM Motors In-Wheel Motors and Electric Drive Solutions. Available online: https://www.gemmotors.si/products/#gem-g-3 (accessed on 10 February 2023).
49. Endurance—Lordstown Motors. Available online: https://www.lordstownmotors.com/pages/endurance (accessed on 9 February 2023).
50. Lordstown "Endurance"—The World's First All-Electric Commercial Pickup Truck—Elaphe. Available online: https://in-wheel.com/en/news/lordstown-endurance-the-worlds-first-all-electric-commercial-pickup-truck/ (accessed on 1 January 2020).
51. Deng, W.; Zuo, S. Axial force and vibroacoustic analysis of external-rotor axial-flux motors. *IEEE Trans. Ind. Electron.* **2018**, *65*, 2018–2030. [CrossRef]
52. Hattori, A.; Noguchi, T.; Kamiyama, H. High-Torque Density Design of Small Motors for Automotive Applications with Double Axial-Air-Gap Structures. *Energies* **2022**, *15*, 7341. [CrossRef]
53. Torkaman, H.; Ghaheri, A.; Keyhani, A. Axial flux switched reluctance machines: a comprehensive review of design and topologies. *IET Electr. Power Appl.* **2019**, *13*, 310–321. [CrossRef]

54. Petrov, I.; Lindh, P.; Peng, W.Y.; Jang, C.S.; Yang, H.P.; Pyrhonen, J. Improvement of axial flux single-rotor single-stator induction machine performance by applying semi-magnetic wedges. In Proceedings of the 2016 22nd International Conference on Electrical Machines, ICEM 2016, Lausanne, Switzerland, 4–7 September 2016; pp. 1795–1800. [CrossRef]
55. Arthur, B.P.B.; Baskaran, U. Improved air-gap flux in axial flux induction machine through shaping of radial slot opening. *Sadhana Acad. Proc. Eng. Sci.* **2020**, *45*, 1–12. [CrossRef]
56. Arabul, F.K.; Senol, I.; Oner, Y. Performance Analysis of Axial-Flux Induction Motor with Skewed Rotor. *Energies* **2020**, *13*, 4991. [CrossRef]
57. Nishanth, F.N.; Verdeghem, J.V.; Severson, E.L. Recent Advances in Analysis and Design of Axial Flux Permanent Magnet Electric Machines. In Proceedings of the 2021 IEEE Energy Conversion Congress and Exposition, ECCE 2021, Virtual, 10–14 October 2021; pp. 3745–3752. [CrossRef]
58. Nobahari, A.; Darabi, A.; Hassannia, A. Various skewing arrangements and relative position of dual rotor of an axial flux induction motor, modelling and performance evaluation. *IET Electr. Power Appl.* **2018**, *12*, 575–580. [CrossRef]
59. Parviainen, A.; Niemelä, M.; Pyrhönen, J. Modeling of axial flux permanent-magnet machines. *IEEE Trans. Ind. Appl.* **2004**, *40*, 1333–1340. [CrossRef]
60. Ma, J.; Qu, R.; Li, J. Optimal design of axial flux switched reluctance motor for electric vehicle application. In Proceedings of the 2014 17th International Conference on Electrical Machines and Systems (ICEMS), Hangzhou, China, 22–25 October 2014; pp. 1860–1865. [CrossRef]
61. Hao, Z.; Ma, Y.; Wang, P.; Luo, G.; Chen, Y. A Review of Axial-Flux Permanent-Magnet Motors: Topological Structures, Design, Optimization and Control Techniques. *Machine* **2022**, *10*, 1178. [CrossRef]
62. High Power Electric Car Motor | High Torque E-Motor | Yasa 750 | YASA. Available online: https://www.yasa.com/products/yasa-750/ (accessed on 8 February 2023).
63. Camilleri, R.; Woolmer, T.; Court, A.; McCulloch, M.D. Investigation into the temperature profile of a liquid cooled YASA© AFPM machine. *IET Conf. Publ.* **2012**, *2012*, 281. [CrossRef]
64. Turntide Technologies Acquires Electric Vehicle Component Developer Avid Technology—Turntide Technologies. Available online: https://turntide.com/press/turntide-technologies-acquires-electric-vehicle-component-developer-avid-technology/ (accessed on 10 February 2023).
65. Magnax—Yokeless Axial Flux Technology. Available online: https://www.magnax.com/ (accessed on 10 February 2023).
66. Electrification—Turntide Technologies. Available online: https://turntide.com/technology/electrification/#ev-motors (accessed on 10 February 2023).
67. EMRAX- E-MOTORS. Available online: https://emrax.com/e-motors/ (accessed on 10 February 2023).
68. Lehr, M.; Reis, K.; Binder, A. Comparison of axial flux and radial flux machines for the use in wheel hub drives. *Elektrotech. Informationstec.* **2015**, *132*, 25–32. [CrossRef]
69. Han, P.; Heins, G.; Zhang, Y.; Ionel, D.M. Integrated Modular Motor Drives Based on Multiphase Axial-flux PM Machines with Fractional-slot Concentrated Windings. In Proceedings of the 2021 IEEE International Electric Machines and Drives Conference, IEMDC 2021, Hartford, CT, USA, 17–20 May 2021. [CrossRef]
70. Abebe, R.; Vakil, G.; Calzo, G.L.; Cox, T.; Lambert, S.; Johnson, M.; Gerada, C.; Mecrow, B. Integrated motor drives: State of the art and future trends. *IET Electr. Power Appl.* **2016**, *10*, 757–771. [CrossRef]
71. Maerz, M.; Poech, M.; Schimanek, E.; Schletz, A. Mechatronic integration into the hybrid powertrain—The thermal challenge. In Proceedings of the International Conference Automotive Power Electronics (APE), Tegernsee, Germany, 4–6 October 2006.
72. Lee, W.; Li, S.; Han, D.; Sarlioglu, B.; Minav, T.A.; Pietola, M. A Review of Integrated Motor Drive and Wide-Bandgap Power Electronics for High-Performance Electro-Hydrostatic Actuators. *IEEE Trans. Transp. Electrif.* **2018**, *4*, 684–693. [CrossRef]
73. Wu, S.; Zhou, J.; Zhang, X.; Yu, J. Design and Research on High Power Density Motor of Integrated Motor Drive System for Electric Vehicles. *Energies* **2022**, *15*, 3542. [CrossRef]
74. Zhang, B.; Song, Z.; Liu, S.; Huang, R.; Liu, C. Overview of Integrated Electric Motor Drives: Opportunities and Challenges. *Energies* **2022**, *15*, 8299. [CrossRef]
75. Jahns, T.M.; Sarlioglu, B. The Incredible Shrinking Motor Drive: Accelerating the Transition to Integrated Motor Drives. *IEEE Power Electron. Mag.* **2020**, *7*, 18–27. [CrossRef]
76. Mohamed, A.H.; Vansompel, H.; Sergeant, P. An Integrated Motor Drive with Enhanced Power Density Using Modular Converter Structure. In Proceedings of the 2021 IEEE International Electric Machines and Drives Conference, IEMDC 2021, Hartford, CT, USA, 17–20 May 2021. [CrossRef]
77. Kim, S.C.; Kim, W.; Kim, M.S. Cooling performance of 25 kW in-wheel motor for electric vehicles. *Int. J. Automot. Technol.* **2013**, *14*, 559–567. [CrossRef]
78. Winterborne, D.; Stannard, N.; Sjoberg, L.; Atkinson, G. An air-cooled yasa motor for in-wheel electric vehicle applications. In Proceedings of the 2019 IEEE International Electric Machines and Drives Conference, IEMDC 2019, San Diego, CA, USA, 12–15 May 2019; pp. 976–981. [CrossRef]
79. Park, M.H.; Kim, S.C. Thermal characteristics and effects of oil spray cooling on in-wheel motors in electric vehicles. *Appl. Therm. Eng.* **2019**, *152*, 582–593. [CrossRef]
80. Lim, D.H.; Kim, S.C. Thermal performance of oil spray cooling system for in-wheel motor in electric vehicles. *Appl. Therm. Eng.* **2014**, *63*, 577–587. [CrossRef]

81. Saleem, A.; Hyeon Park, M.; Ambreen, T.; Chul Kim, S. Optimization of oil flow distribution inside the in-wheel motor assembly of electric vehicles for improved thermal performance. *Appl. Therm. Eng.* **2022**, *201*, 117753. [CrossRef]
82. Acquaviva, A.; Skoog, S.; Thiringer, T. Design and Verification of In-Slot Oil-Cooled Tooth Coil Winding PM Machine for Traction Application. *IEEE Trans. Ind. Electron.* **2021**, *68*, 3719–3727. [CrossRef]
83. Marcolini, F.; Donato, G.D.; Caricchi, F. Direct oil cooling of end-windings in torus-type axial-flux permanent-magnet machines. In Proceedings of the 2019 IEEE Energy Conversion Congress and Exposition, ECCE 2019, Baltimore, MD, USA, 29 September–3 October 2019; pp. 5645–5651. [CrossRef]
84. Chattopadhyay, R.; Islam, M.S.; Jung, J.; Mikail, R.; Husain, I. Winding Embedded Liquid Cooling for Slotless Motors in Transportation Applications. *IEEE Trans. Ind. Appl.* **2022**, *58*, 7110–7120. [CrossRef]
85. Liang, P.; Chai, F.; Shen, K.; Liu, W. Water Jacket and Slot Optimization of a Water-Cooling Permanent Magnet Synchronous In-Wheel Motor. *IEEE Trans. Ind. Appl.* **2021**, *57*, 2431–2439. [CrossRef]
86. Satrústegui, M.; Martinez-Iturralde, M.; Ramos, J.C.; Gonzalez, P.; Astarbe, G.; Elosegui, I. Design criteria for water cooled systems of induction machines. *Appl. Therm. Eng.* **2017**, *114*, 1018–1028. [CrossRef]
87. Fan, P.; Fan, D.; Zhu, X.; Xiang, Z.; Zhou, X. Research on Heat Dissipation Characteristics of PM in-wheel Motor Using Electrical-Thermal Bi-Directional Coupling Method. In Proceedings of the 2022 IEEE Transportation Electrification Conference and Expo, Asia-Pacific, ITEC Asia-Pacific 2022, Haining, China, 28–31 October 2022. [CrossRef]
88. Wang, Q.; Li, R.; Zhao, Z.; Liang, K.; Xu, W.; Zhao, P. Temperature Field Analysis and Cooling Structure Optimization for Integrated Permanent Magnet In-Wheel Motor Based on Electromagnetic-Thermal Coupling. *Energies* **2023**, *16*, 1527. [CrossRef]
89. Pillay, P.; Krishnan, R. Modeling, Simulation, and Analysis of Permanent-Magnet Motor Drives, Part I: The Permanent-Magnet Synchronous Motor Drive. *IEEE Trans. Ind. Appl.* **1989**, *25*, 265–273. [CrossRef]
90. Bida, V.M.; Samokhvalov, D.V.; Al-Mahturi, F.S. PMSM vector control techniques—A survey. In Proceedings of the 2018 IEEE Conference of Russian Young Researchers in Electrical and Electronic Engineering, ElConRus 2018, St. Petersburg, Russia, 29 January–1 February 2018; pp. 577–581. [CrossRef]
91. Guo, Z.; Zhang, J.; Sun, Z.; Zheng, C. Indirect Field Oriented Control of Three-phase Induction Motor Based on Current-source Inverter. *Procedia Eng.* **2017**, *174*, 588–594. [CrossRef]
92. Pedrosa, D.; Carvalho, J.; Goncalves, H.; Monteiro, V.; Fernandes, A.; Afonso, J.L. Field oriented control of an axial flux permanent magnet synchronous motor for traction solutions. In Proceedings of the IECON (Industrial Electronics Conference), Dallas, TX, USA, 29 October–1 November 2014; pp. 1466–1472. [CrossRef]
93. Pedrosa, D.; Peixoto, H.; Goncalves, H.; Martins, J.S.; Couto, C.; Afonso, J.L. FPGA field oriented control of an Axial Flux motor-in-wheel. In Proceedings of the IECON (Industrial Electronics Conference), Dallas, TX, USA, 29 October–1 November 2014; pp. 594–600. [CrossRef]
94. Buja, G.S.; Kazmierkowski, M.P. Direct torque control of PWM inverter-fed AC motors—A survey. *IEEE Trans. Ind. Electron.* **2004**, *51*, 744–757. [CrossRef]
95. Aktas, M.; Awaili, K.; Ehsani, M.; Arisoy, A. Direct torque control versus indirect field-oriented control of induction motors for electric vehicle applications. *Eng. Sci. Technol. Int. J.* **2020**, *23*, 1134–1143. [CrossRef]
96. Malyshev, A.; Ivanov, A. Direct Torque Control of the Axial Flux Permanent Magnet Motor. In Proceedings of the 13th International IEEE Scientific and Technical Conference Dynamics of Systems, Mechanisms and Machines, Dynamics 2019, Omsk, Russia, 5–7 November 2019. [CrossRef]
97. Lin, C.; Liang, S.; Chen, J.; Gao, X. A multi-objective optimal torque distribution strategy for four in-wheel-motor drive electric vehicles. *IEEE Access* **2019**, *7*, 64627–64640. [CrossRef]
98. Zhou, H.; Jia, F.; Jing, H.; Liu, Z.; Güvenç, L. Coordinated Longitudinal and Lateral Motion Control for Four Wheel Independent Motor-Drive Electric Vehicle. *IEEE Trans. Veh. Technol.* **2018**, *67*, 3782–3790. [CrossRef]
99. Cai, L.; Liao, Z.; Wei, S.; Li, J. Novel Direct Yaw Moment Control of Multi-Wheel Hub Motor Driven Vehicles for Improving Mobility and Stability. *IEEE Trans. Ind. Appl.* **2022**, *59*, 591–600. [CrossRef]
100. Tristano, M.; Lenzo, B.; Xu, X.; Forrier, B.; D'Hondt, T.; Risaliti, E.; Wilhelm, E. Real-time implementation of yaw rate and sideslip control through individual wheel torques. In Proceedings of the 2022 IEEE Vehicle Power and Propulsion Conference, VPPC 2022, Merced, CA, USA, 1–4 November 2022. [CrossRef]
101. Asiabar, A.N.; Kazemi, R. A direct yaw moment controller for a four in-wheel motor drive electric vehicle using adaptive sliding mode control. *Proc. Inst. Mech. Eng. Part K: J. Multi-Body Dyn.* **2019**, *233*, 549–567. [CrossRef]
102. Oraby, W.A.H.; El-Demerdash, S.M.; Selim, A.M.; Faizz, A.; Crolla, D.A. Improvement of Vehicle Lateral Dynamics by Active Front Steering Control. *SAE Trans.* **2004**, *113*, 1101–1110.
103. Cui, F.L.; Ge, P.S.; Wang, Y.; Zhang, T. Active Front Steering Controller for Distributed Drive Electric Vehicles based on Sliding Mode Control. In Proceedings of the 2022 6th CAA International Conference on Vehicular Control and Intelligence, CVCI 2022, Nanjing, China, 28–30 October 2022. [CrossRef]
104. Tian, T.; Fang, L.; Ding, S.; Zheng, W.X. Adaptive Fuzzy Sliding Mode Control for Active Front Steering System. In Proceedings of the Chinese Control Conference, CCC, Shenyang, China, 27–29 July 2020; pp. 358–363. [CrossRef]
105. Wang, L.; Liu, G.; Zhang, D.; Miao, P. Integrated control of active front steering and direct yaw moment for multi-wheel independently driven electric vehicles. In Proceedings of the 2013 International Conference on Electrical Machines and Systems, ICEMS 2013, Busan, Republic of Korea, 26–29 October 2013; pp. 2301–2304. [CrossRef]

106. Li, S.; Yang, Z. AFS/DYC Control of In-Wheel Motor Drive Electric Vehicle with Adaptive Tire Cornering Stiffness. In Proceedings of the 2022 6th CAA International Conference on Vehicular Control and Intelligence, CVCI 2022, Nanjing, China, 28–30 October 2022. [CrossRef]
107. Guo, J.; Luo, Y.; Li, K. An adaptive hierarchical trajectory following control approach of autonomous four-wheel independent drive electric vehicles. *IEEE Trans. Intell. Transp. Syst.* **2018**, *19*, 2482–2492. [CrossRef]
108. Liu, H.; Liu, C.; Han, L.; Xiang, C. Handling and Stability Integrated Control of AFS and DYC for Distributed Drive Electric Vehicles Based on Risk Assessment and Prediction. *IEEE Trans. Intell. Transp. Syst.* **2022**, *23*, 23148–23163. [CrossRef]
109. Xu, Y.; Jiang, L.; Wei, B.; Qiu, L. An Optimal Torque Distribution Strategy for Four-Motorized-Wheel Electric Vehicle Considering Energy Conversation. *IEEE Access* **2020**, *8*, 135975–135988. [CrossRef]
110. He, S.; Fan, X.; Wang, Q.; Chen, X.; Zhu, S. Review on Torque Distribution Scheme of Four-Wheel In-Wheel Motor Electric Vehicle. *Machines* **2022**, *10*, 619. [CrossRef]
111. Lin, C.; Xu, Z. Wheel Torque Distribution of Four-Wheel-Drive Electric Vehicles Based on Multi-Objective Optimization. *Energies* **2015**, *8*, 3815–3831. [CrossRef]
112. Saiteja, P.; Ashok, B.; Wagh, A.S.; Farrag, M.E. Critical review on optimal regenerative braking control system architecture, calibration parameters and development challenges for EVs. *Int. J. Energy Res.* **2022**, *46*, 20146–20179. [CrossRef]
113. Guo, L.; Xu, H.; Zou, J.; Jie, H.; Zheng, G. Torque Distribution Strategy of Four-Wheel Independent Drive Electric Vehicle Based on Optimal Energy Consumption. In Proceedings of the 2020 IEEE 3rd International Conference on Electronics Technology, ICET 2020, Chengdu, China, 8–11 May 2020; pp. 252–256. [CrossRef]
114. De Klerk, M.L.; Saha, A.K. A Comprehensive Review of Advanced Traction Motor Control Techniques Suitable for Electric Vehicle Applications. *IEEE Access* **2021**, *9*, 125080–125108. [CrossRef]
115. Liang, J.; Feng, J.; Fang, Z.; Lu, Y.; Yin, G.; Mao, X.; Wu, J.; Wang, F. An Energy-oriented Torque-vector Control Framework for Distributed Drive Electric Vehicles. *IEEE Trans. Transp. Electrif.* **2023**. [CrossRef]
116. Sun, X.; Shi, Z.; Cai, Y.; Lei, G.; Guo, Y.; Zhu, J. Driving-Cycle-Oriented Design Optimization of a Permanent Magnet Hub Motor Drive System for a Four-Wheel-Drive Electric Vehicle. *IEEE Trans. Transp. Electrif.* **2020**, *6*, 1115–1125. [CrossRef]
117. Shi, Z.; Sun, X.; Lei, G.; Tian, X.; Guo, Y.; Zhu, J. Multiobjective Optimization of a Five-Phase Bearingless Permanent Magnet Motor Considering Winding Area. *IEEE/ASME Trans. Mechatronics* **2022**, *27*, 2657–2666. [CrossRef]
118. Sun, X.; Xu, N.; Yao, M. Sequential Subspace Optimization Design of a Dual Three-Phase Permanent Magnet Synchronous Hub Motor Based on NSGA III. *IEEE Trans. Transp. Electrif.* **2023**, *9*, 622–630. [CrossRef]
119. Anderson, M.J. Unsprung Mass with In-Wheel Motors-Myths and Realities. 2010. Available online: https://www.proteanelectric.com/f/2018/04/protean-Services3.pdf (accessed on 20 March 2023).
120. Nie, S.; Zhuang, Y.; Chen, F.; Wang, Y.; Liu, S. A method to eliminate unsprung adverse effect of in-wheel motor-driven vehicles. *J. Low Freq. Noise Vib. Act. Control.* **2018**, *37*, 955–976. [CrossRef]
121. Quynh, L.V.; Cuong, B.V.; Liem, N.V.; Long, L.X.; Dung, P.T.T. Effect of in-wheel motor suspension system on electric vehicle ride comfort. *Vibroeng. Procedia* **2019**, *29*, 148–152. [CrossRef]
122. Zhao, Z.; Taghavifar, H.; Du, H.; Qin, Y.; Dong, M.; Gu, L. In-Wheel Motor Vibration Control for Distributed-Driven Electric Vehicles: A Review. *IEEE Trans. Transp. Electrif.* **2021**, *7*, 2864–2880. [CrossRef]
123. Li, Z.; Zheng, L.; Ren, Y.; Li, Y.; Xiong, Z. Multi-objective optimization of active suspension system in electric vehicle with In-Wheel-Motor against the negative electromechanical coupling effects. *Mech. Syst. Signal Process.* **2019**, *116*, 545–565. [CrossRef]
124. Yu, Y.; Zhao, L.; Zhou, C. Influence of Rotor-Bearing Coupling Vibration on Dynamic Behavior of Electric Vehicle Driven by In-Wheel Motor. *IEEE Access* **2019**, *7*, 63540–63549. [CrossRef]
125. Biček, M.; Connes, R.; Omerović, S.; Gündüz, A.; Kunc, R.; Zupan, S. The Bearing Stiffness Effect on In-Wheel Motors. *Sustainability* **2020**, *12*, 4070. [CrossRef]
126. Biček, M.; Lampič, G.; Zupan, S.; Obrul, B.; Gotovac, G.; Štefe, B.; Valentinčič, J. High torque in-wheel motors for rescue vehicles. In Proceedings of the Innovative Automotive Technology—IAT, Nova Gorica, Slovenia, 12–13 April 2012; pp. 1–14.
127. Biček, M.; Pepelnjak, T.; Pušavec, F. Production aspect of direct drive in-wheel motors. *Procedia CIRP* **2019**, *81*, 1278–1283. [CrossRef]
128. Biček, M.; Kunc, R.; Zupan, S. Mechanical Impact on In-Wheel Motor's Performance. *J. Mech.* **2017**, *33*, 607–618. [CrossRef]
129. Galeazzi, A.; Roberts, G. Influence of wheel bearing performance on In-wheel motor advanced applications. In Proceedings of the 2013 World Electric Vehicle Symposium and Exhibition, EVS 2014, Barcelona, Spain, 17–20 November 2013. [CrossRef]
130. Kostic Perovic, D. Making the Impossible, Possible—Overcoming the Design Challenges of In Wheel Motors. *World Electr. Veh. J.* **2012**, *5*, 514–519. [CrossRef]
131. Wheel Hub Motor and Method for Sealing a Wheel Hub Motor. 2013. Available online: https://patents.google.com/patent/WO2014108231A2/en (accessed on 23 February 2023).
132. Materials and Grades—Amazing Magnets. Available online: https://amazingmagnets.com/magnetic-grade-chart/ (accessed on 23 February 2023).
133. Gauß, R.; Burkhardt, C.; Carencotte, F.; Gasparon, M.; Gutfleisch, O.; Higgins, I.; Karajić, M.; Klossek, A.; Mäkinen, M.; Schäfer, B.; et al. *Rare Earth Magnets and Motors: A European Call for Action*; Technical Report; European Raw Materials Alliance: Berlin, Germany, 2021.

134. Cui, J.; Kramer, M.; Zhou, L.; Liu, F.; Gabay, A.; Hadjipanayis, G.; Balasubramanian, B.; Sellmyer, D. Current progress and future challenges in rare-earth-free permanent magnets. *Acta Mater.* **2018**, *158*, 118–137. [CrossRef]
135. Rare Earths: Mine Production Top Countries 2022 | Statista. Available online: https://www.statista.com/statistics/268011/top-countries-in-rare-earth-mine-production/ (accessed on 23 February 2023).
136. refreedrive | Rare Earth Free E-Drives Featuring Low Cost Manufacturing. Available online: https://www.refreedrive.eu/ (accessed on 21 February 2023).
137. Fujimoto, H.; Shimizu, O.; Nagai, S.; Fujita, T.; Gunji, D.; Ohmori, Y. Development of wireless in-wheel motors for dynamic charging: From 2nd to 3rd generation. In Proceedings of the 2020 IEEE PELS Workshop on Emerging Technologies: Wireless Power Transfer, WoW 2020, Seoul, Republic of Korea, 15–19 November 2020; pp. 56–61. [CrossRef]
138. Chen, Y.; Fu, W.; Weng, X. A Concept of General Flux-Modulated Electric Machines Based on a Unified Theory and Its Application to Developing a Novel Doubly-Fed Dual-Stator Motor. *IEEE Trans. Ind. Electron.* **2017**, *64*, 9914–9923. [CrossRef]
139. Ruiz-Ponce, G.; Arjona, M.A.; Hernandez, C.; Escarela-Perez, R. A Review of Magnetic Gear Technologies Used in Mechanical Power Transmission. *Energies* **2023**, *16*, 1721. [CrossRef]
140. Jing, L.; Gong, J.; Huang, Z.; Ben, T.; Huang, Y. A New Structure for the Magnetic Gear. *IEEE Access* **2019**, *7*, 75550–75555. [CrossRef]
141. Li, W.; Chau, K.T.; Jiang, J.Z. Application of linear magnetic gears for pseudo-direct-drive oceanic wave energy harvesting. *IEEE Trans. Magn.* **2011**, *47*, 2624–2627. [CrossRef]
142. Atallah, K.; Calverley, S.D.; Howe, D. Design, analysis and realisation of a high-performance magnetic gear. *IEE Proc. Electr. Power Appl.* **2004**, *151*, 135–143. [CrossRef]
143. Gardner, M.C.; Jack, B.E.; Johnson, M.; Toliyat, H.A. Comparison of Surface Mounted Permanent Magnet Coaxial Radial Flux Magnetic Gears Independently Optimized for Volume, Cost, and Mass. *IEEE Trans. Ind. Appl.* **2018**, *54*, 2237–2245. [CrossRef]
144. Magnetic Geared Machine | HQ Magnet. Available online: https://hq-magnet.com/magnetic-geared-machine/ (accessed on 23 February 2023).
145. Wu, F.; El-Refaie, A.M. Permanent magnet vernier machine: A review. *IET Electr. Power Appl.* **2019**, *13*, 127–137. [CrossRef]
146. Li, D.; Qu, R.; Li, J.; Xu, W. Consequent-Pole Toroidal-Winding Outer-Rotor Vernier Permanent-Magnet Machines. *IEEE Trans. Ind. Appl.* **2015**, *51*, 4470–4481. [CrossRef]
147. Lee, C.H.; Angle, M.; Bhalla, K.K.; Qasim, M.; Mei, J.; Mohammadi, S.; Iyer, K.L.V.; Sinkular, J.J.; Kirtley, J.L. Quantitative Comparison of Vernier Permanent-Magnet Motors with Interior Permanent-Magnet Motor for Hybrid Electric Vehicles. *Energies* **2018**, *11*, 2546. [CrossRef]
148. Shafiei, S.; Noroozi, M.A.; Milimonfared, J.; Lesani, H. Performance Comparison of Outer Rotor Permanent Magnet Vernier Motor for Direct Drive Systems. In Proceedings of the 2020 11th Power Electronics, Drive Systems, and Technologies Conference, PEDSTC 2020, Tehran, Iran, 4–6 February 2020. [CrossRef]
149. Hosoya, R.; Shimomura, S. Apply to in-wheel machine of permanent magnet vernier machine using NdFeB bonded magnet Fundamental study. In Proceedings of the 8th International Conference on Power Electronics—ECCE Asia: "Green World with Power Electronics", ICPE 2011-ECCE Asia, Jeju, Republic of Korea, 30 May–3 June 2011; pp. 2208–2215. [CrossRef]
150. Wu, W.; Xu, L.; Liu, B. Design, Analysis, and Optimization of Permanent Magnet Vernier Machines Considering Rotor Losses. *Energies* **2022**, *15*, 1502. [CrossRef]
151. Li, J.; Wu, D.; Zhang, X.; Gao, S. A new permanent-magnet vernier in-wheel motor for electric vehicles. In Proceedings of the 2010 IEEE Vehicle Power and Propulsion Conference, VPPC 2010, Lille, France, 1–3 September 2010. [CrossRef]
152. Zhu, X.; Zhao, W.; Zhu, J.; Bian, F. A high power factor fault-tolerant vernier permanent-magnet machine. *AIP Adv.* **2017**, *7*, 056622. [CrossRef]